western australian marine science institution

Physical oceanographic dynamics in the Kimberley

Gregory Ivey[1], Richard Brinkman[2], Ryan Lowe[1], Nicole Jones[1], Graham Symonds[3], Alexis Espinosa-Gayosso[1]

[1]*University of Western Australia, Crawley, Western Australia*

[2]*Australian Institute of Marine Science, Townsville, Queensland*

[3]*CSIRO, Floreat, Western Australia*

WAMSI Kimberley Marine Research Program

Final Report

Project 2.2.1

December 2016

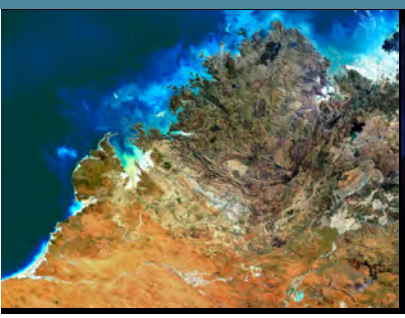
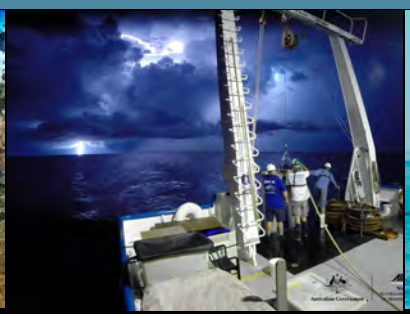
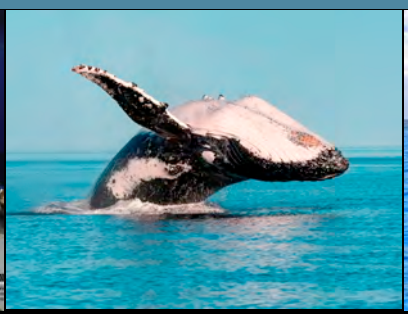
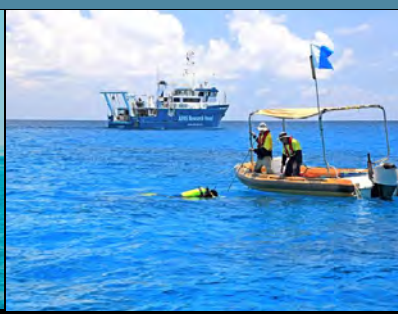

western australian marine science institution

THE UNIVERSITY OF WESTERN AUSTRALIA

Australian Government

Australian Institute of Marine Science

CSIRO

WAMSI Kimberley Marine Research Program

Initiated with the support of the State Government as part of the Kimberley Science and Conservation Strategy, the Kimberley Marine Research Program is co-invested by the WAMSI partners to provide regional understanding and baseline knowledge about the Kimberley marine environment. The program has been created in response to the extraordinary, unspoilt wilderness value of the Kimberley and increasing pressure for development in this region. The purpose is to provide science based information to support decision making in relation to the Kimberley marine park network, other conservation activities and future development proposals.

Front cover images (L-R)

Image 1: Satellite image of the Kimberley coastline

Image 2: Late night sampling on RV Solander with distant thunderstorm, Collier Bay, February 2014 (R. Brinkman, AIMS)

Image 3: Humpback whale breaching, Exmouth (Image: Pam Osborn)

Image 4: Diving tender with RV Solander in Collier Bay, November 2015 (J. Rasmussen, AIMS)

Year of publication: September 2016

Metadata: http://catalogue.aodn.org.au/geonetwork/srv/eng/metadata.show?uuid=6b182cf6-fa72-4ab4-a92a-c9d4b0dcbe4f

Citation: Ivey G, Brinkman R, Lowe R, Jones N, Symonds G, Espinosa-Gayosso A (2016) Physical oceanographic dynamics in the Kimberley. Report of Project 2.2.1 prepared for the Kimberley Marine Research Program, Western Australian Marine Science Institution, Perth, Western Australia, 43pp.

Author Contributions: GI, RB, Rl and NJ designed the field experiments, GI, RB, RL, NJ, GS and A E-G conducted the field work and the data analysis, A E-G, GI, RL and NJ conducted the numerical modeling, and GI, RB, RL, NJ, GS and A E-G contributed to the report and wrote the related manuscripts.

Corresponding author and Institution: Greg Ivey, The University of Western Australia, greg.ivey@uwa.edu.au.

Funding Sources: This project was funded (commissioned) by the Western Australian Marine Science Institution (WAMSI) as part of the WAMSI Kimberley Marine Research Program, a $30M program with seed funding of $12M provided by State government as part of the Kimberley Science and Conservation Strategy. The Program has been made possible through co-investment from the WAMSI Joint Venture partners. Additional funding was provided by Australian Research Council (ARC) Future Fellowship grant (FT110100201) to RJL.

Competing Interests: The commercial investors and data providers had no role in the data analysis, data interpretation, the decision to publish or in the preparation of manuscripts. The authors have declared that no competing interests exists.

Kimberley Traditional Owner agreement: This research was enabled by the Traditional Owners through their advice, participation and consent to access their traditional lands.

Acknowledgements: Our team would like to acknowledge the Bardi Jawi people, the Traditional Owners both past and present, who continue to care for this country. We thank the skipper and crew of AIMS RV Solander who made the field work possible. Thomas Nguyen, Renee Gruber, Edwin Drost, Alexis Espinosa-Gayossa and Eric Raies provided invaluable field assistance.

Collection permits/ethics approval: No collection occurred in the production of this report.

Contents

Executive summary

The overall objectives of Project 2.2.1 were to quantify the physical oceanographic dynamics in the coastal Kimberley region by undertaking both a field observational program and development of a field-validated three-dimensional hydrodynamic model with domain extending from the coast to the shelf waters. These integrated approaches would enable detailed understanding of the primarily tidally-driven dynamics in the region including the transport pathways, exchange rates and flushing processes. The project provides insight into the role of the catchment versus the open ocean in the physical and hence coastal ecosystem dynamics.

On a localized reef scale, an intensive field study on Tallon Reef and associated hydrodynamic theory has quantified the flow fields over intertidal reef platforms. A key feature of the over-reef flows is the large asymmetries on the ebb and flood phases. On the ebb phase, the reef drainage time-scale is long and dependent on the reef morphology, tidal range and friction associated with the bottom roughness. Reefs in the area have evolved such that this reef drainage time-scale is long compared to the tidal period. This provides physical insight into how the very productive reef ecosystems living within the intertidal zone of reefs in the Kimberley, and high above the offshore low tide elevation, can remain submerged (and hence survive) over a full tidal cycle.

On the regional scale, the Collier Bay/Camden Sound region was chosen as representative of the western Kimberley area that experiences the most extreme tidal range. The field observational program in this region involved two components. The first was the deployment and long-term maintenance of three oceanographic moorings in Collier Bay/Camden Sound over an annual cycle at the inner, mid and outer shelf regions. And the second component was two ten-day process-oriented research cruises on AIMS RV Solander, one in the dry season and one in the wet season. These were conducted to provide high-resolution time and space observations of key physical processes in the two contrasting seasons. A Regional Ocean Modelling Systems (ROMS) three-dimensional hydrodynamic model for the Camden Sound/Collier Bay region was developed. A key aspect of the project is that the model performance has been validated using the field observations, in particular using the moorings placed at the three shelf regions. These results have been passed over to project 2.2.2 (Biogeochemistry) to guide their interpretation of measurements and modelling of the biological oceanography of the region.

This project has shown that in the coastal Kimberley waters the effects of wind-forcing and baroclinic forcing, due to density differences between fresh water input from the coast and offshore ocean waters, are both of only secondary importance while the dominant forcing is the tide, in particular the M2 tide with a 12.4hr period. The strong tidal forcing and associated turbulence generated by the tidally-forced flow moving over the hydraulically rough bottom ensures the water column is vertically near well-mixed over the entire annual cycle, in water depths up to approximately 50m. The macrotidal forcing, with tidal amplitudes up to 12m, and the complex topography/bathymetry of islands and reefs, are the two dominant factors that control horizontal circulation with, in some locations, depth-averaged instantaneous currents reaching as high as 3 m/s.

Despite the very large instantaneous currents, it is the tidal currents averaged over a full tidal period that are key to the net circulation. Due to the flow restrictions of the reef/island channels, highly energetic jets can be locally generated at each tidal cycle, which reverse direction every tidal cycle and locally pump water masses (and suspended or biological matter) both in and out of the coastal region. The asymmetry of this tidal pumping is the underlying mechanism that drives the complex net or residual circulations and the spatial pattern of this residual circulation strongly reflects the underlying topography/bathymetry. Residual depth-averaged velocities can reach as high as 1 m/s, particularly over shallow reefs and in narrow channels, but bay-scale residual currents are typically of the order of 1 cm/s. While the residual circulation is highly spatially variable, the numerical model shows that in Camden Sound/Collier Bay the residual currents form a slow anti-clockwise residual circulation with oceanic water entering from the west and exiting towards the northeast.

This tidally-dominated complex residual circulation drives flushing and the mechanisms and exchange times vary across Camden Sound/Collier Bay. The dry season occupies most of the annual cycle and the mechanism of

flushing is the entry of open ocean water entering and diluting the coastal waters. The flushing times vary strongly across the Bay: from less than 20 days on the western side, between 60-80 days for the central region, and up to 120-140 days for the eastern side and the small coastal estuaries. Thus there is a near 7-fold variation in flushing across the Bay, but the Bay-scale average flushing times is around 60-80 days. During the wet season some regions are additionally flushed by fresh water input from the catchment, reducing local flushing times by up to 50%, but this is strongly dependent on the location, and the duration and intensity of the inflows from the catchment which are controlled by the aperiodic rainfall events.

The description of the physical oceanographic dynamics in the coastal Kimberley resulting from this study, in turn, strongly influences the biological processes described in Project 2.2.2 and other parts of the KMRP.

Implications for management

From the two major field trips, there is detailed spatial information on physical oceanic properties during wet and dry seasons obtained from both ship-based survey and the long term continuous measurements at the three sites on the inner, mid and outer shelf locations in the Collier Bay region.

These data provide a characterization of the oceanographic processes for the western Kimberley region and a unique resource for management application including:

- assessment of local dispersion/mixing processes to better understand ecological processes such as connectivity or recruitment, both important to the long term health of coral and seagrass habitats; and
- a benchmark for testing and evaluating future model development on differing spatial scales or even different types of models that may be developed for future management purposes, including such specialised applications as predicting the spread of pollutants from an oil spill.

Coupled with the findings from project 2.2.2 and 2.2.6, this characterization of the hydrodynamics of the region can be used to better understand the flow of nutrients and energy through the coastal habitats and ecosystem. This has important implications for the management of habitats and the spatial scale on which they need to be considered for management purposes. For example:

- the understanding of water mixing, flow and influence of the tidal cycle can be used in the evaluation of industrial or other commercial developments, clarifying the realistic area of potential impact and subsequent ramifications for habitat. Other examples of how the model can be used as a tool by managers to address management needs are highlighted below;
- the model output, with predictions of currents, water levels and mixing processes, can be used, to drive ecological models to answer very focused questions regarding, for example, the regional influence of proposed resource or aquaculture development projects; and
- the model provides the hydrodynamic variables needed to drive specialized spill models to assess the spreading and fate of oil and pollutants that may be released into the system at surface or over depth.

Appendix 1 outlines the management questions originally posed for this project and the answers that can be provided at this stage, recognizing that some elements of the questions were well beyond the scope of this study and should be considered as additional residual knowledge gaps.

Products and Tools

The project has built a 3D coastal scale ROMS hydrodynamic numerical model that has been fully validated against the field data. As well as the examples described above, the model can, in turn, be used as a tool for a variety of future management purposes more generally including:

- both hindcasting and forecasting predictions for any period by retaining the dominant (and invariant) tidal forcing, and by inputing the relevant meteorological forcing and, during the wet season, any freshwater input from the catchment; and
- long-term forecasting of response to climate change scenarios, such as sensitivity to changes in offshore ocean properties and/or rainfall in the Kimberley catchment.

Key residual knowledge gaps

The project has focused on the area of the Kimberley with the highest tidal amplitude, namely the Camden Sound/Collier Bay region, and a natural step would be extending the model domain to include the entire Kimberley coastline. In the shallow coastal waters, defined here as depths of 50m and less, high-quality bathymetric information such as channel and reef characteristics are needed to describe the bathymetry in this extended domain. Increasing the overall scale of the model, while retaining the fine resolutions required to understand processes, would require long-term, simultaneous moorings in multiple locations along the coast. Deployment of simultaneous moorings over multiple years would also provide records of aperiodic intense tropical cyclones and thus provide a greater understanding of the short-term variability of the oceanographic processes of the region during the wet season.

1 Introduction

A key to understanding and managing any marine ecosystem is to understand the causes and character of the motion of ocean; the physical oceanographic dynamics. This includes knowledge of the time-varying water levels, the currents and circulation processes, the turbulent mixing, the temperature, salinity and density fields, the role of the underlying bathymetry, and the cumulative effects of these quantities on such detailed issues as open ocean-bay flushing rates and ocean-reef exchange rates. The physics of the ocean are determined by the cumulative effect of a variety of physical forcing processes including: the gravitational pull of the moon and sun force time-varying tides, the meteorological forcing from wind, solar heating and cooling, and density differences in the water due to the difference in density between fresh water from direct rainfall and catchment-derived river inflow and the relatively dense open ocean water.

The Kimberley region is well known as a macrotidal region and the large variation in water surface heights, of up to 12m at spring tidal periods, in combination with the relatively shallow water of the region, drives very strong horizontal currents. In moving over the hydraulically rough bottom, these tidal flows can, in turn, generate very strong turbulent mixing. While this is to be expected in the region, it is not clear what the relative contribution can be from other forcing agents such as wind forcing which has both a background component as well as aperiodic influence from tropical cyclones which can influence the region in the Austral summer months. A key feature of the Kimberley is the very complex coastline and coastal region, with headlands and bays, offshore island and reef systems.

It is not possible within the scope of this project to investigate the entire Kimberley coastal region, but it is important to choose a focus area of study which is representative of the physical complexities of the region, large enough to be influenced by all the key physical processes but also of a scale that can be surveyed with ship-based and a finite number of fixed but long term moorings. Accordingly, the Collier Bay/Camden Sound region was chosen as representative of the Kimberley area and was the focus area of this project, and the project involved a field program followed by a numerical modelling program. The field observational program involved two components. Firstly, the deployment and long-term maintenance of three oceanographic moorings in Collier Bay/Camden Sound over the period October 2013 to August 2014 at inner, mid and outer shelf or Sound locations. Secondly, two ten-day process-oriented research cruises on AIMS RV Solander, one in the dry season and one in the wet season, to provide high-resolution time and space observations of key physical processes in the two contrasting seasons. In the modelling phase, the project developed a Regional Ocean Modelling Systems (ROMS) three-dimensional hydrodynamic model for the Camden Sound/Collier Bay region. The model performance was evaluated and tested using the field observations, particularly the moorings placed at the inner, mid and outer shelf sites. Below we describe the details of firstly the fieldwork program, followed by the numerical modelling component of the project.

2 Materials and Methods

2.1 Field Work

2.1.1 Dry Season Experiment

The field experiment in the Camden Sound/Collier Bay region in the dry season occurred over the period 21 October 2013 to 1 November 2013. This cruise was in support of Projects 2.2.1, 2.2.2 and 2.2.6. The cruise on RV Solander was led by RB from AIMS and covered the region from the outer shelf, into Collier Bay and also Walcott Inlet. Three long-term moorings were deployed, each with sub-surface upward-looking Acoustic Doppler Current Profilers mounted near-bed with additional temperature and salinity loggers, deployed at sites on the outer shelf, middle shelf and inner shelf. A short-term mooring, with a similar configuration of ADCP and temperature and salinity loggers, was deployed in Walcott inlet itself. Continual ADCP transecting and CTD stations were made while the ship was underway, as well as intensive 24 hour measurements at 4 fixed stations in the cruise. As well as physical variables, biological measurements were also made including plankton tows, and zooplankton

production experiments. Figure 1 summarizes the cruise tracks and mooring locations, and full details are in the Appendix 1 AIMS Research Voyage Report Trip 5887.

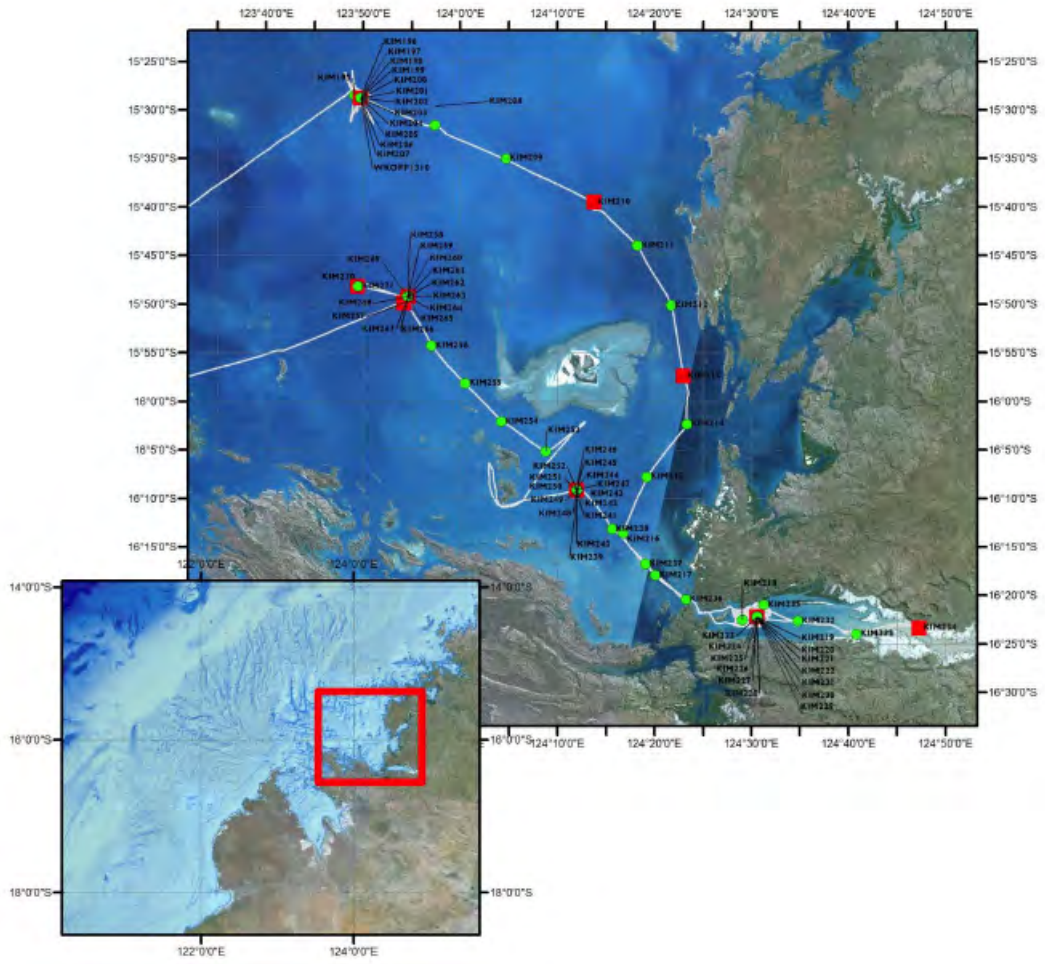

Figure 1 Cruise track and sampling locations for trip 5887. Grey line indicated ship track, green dots show CTD stations, and red squares show plankton new tows. The cluster of stations around 4 sites on the outer, middle and inner shelf, and within Walcott Inlet indicates the site of the 24-hour stations and mooring locations.

2.1.2 Wet Season Experiment

This second field trip during the wet season was from 10 to 21st March 2014 (Figure 2). The geographic focus was along an estuarine-to-offshore transect from Walcott Inlet to outer Collier Bay, with our sampling primarily clustered around 4 sites where we undertook 24 hour sampling (time interval= 2 hours), plus stations spread throughout Collier Bay and Walcott Inlet. We completed 98 sampling stations, all including CTD cast, most including water sampling stations and many including plankton net tows. We completed 8 production experiments, 6 ebb production experiments and a series of light vs photosynthesis experiments. We undertook continual ADCP transecting (along route) and ADCP stations when water sampling/CTD, and mapped surface and sub-surface hydrographic properties through sim-ops of TSG, CTD and ADCP. Three medium-term ADCP moorings deployed at the outer shelf, mid shelf and inner shelf were all recovered, serviced and re-deployed.

Water sampling and CTD profiling was also undertaken in the Isdell River to support WAMSI project 2.2.6.

Due to the transit to Darwin we were also able to reoccupy sampling stations from earlier cruises along the central and Northern Kimberley, and we focused on stations at the entrance to bays/estuaries that receive large riverine inputs. We could not recover the UWA sub-surface ADCP bottom frame in Walcott Inlet due to loss of the surface marker and recovery line. Analysis (primarily QC) of the mooring data is complete. Figure 2 summarizes the cruise tracks and mooring locations, and full details are in the attached AIMS Research Voyage Report Trip 5938.

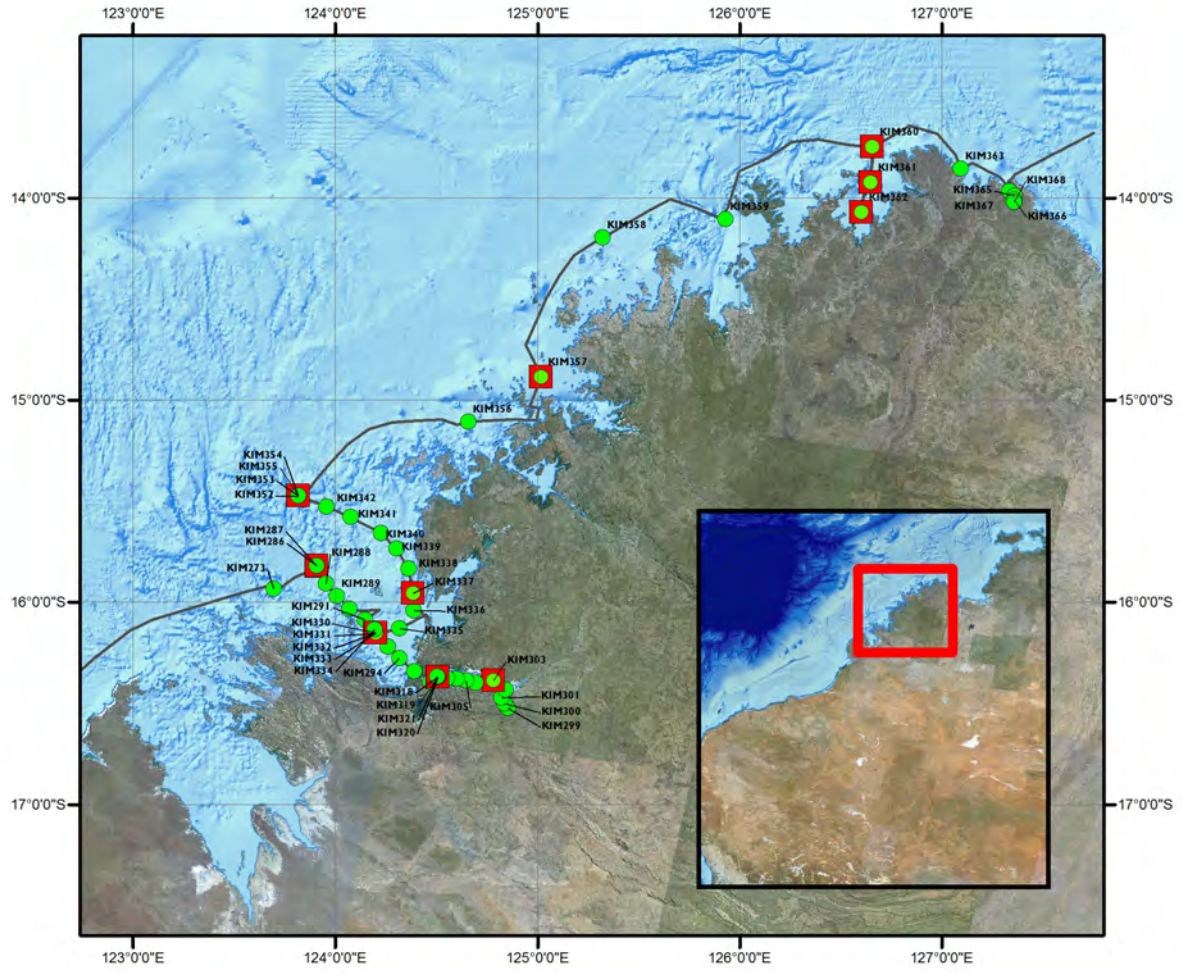

Figure 2 Cruise track and sampling locations for trip 58938. Grey line indicated ship track, green dots show CTD stations, and red squares show plankton net tows.

Final recovery of the 3 ADCP moorings was in August 2014 piggybacking on the last IMOS funded trip to retrieve the IMOS Kimberley moorings.

2.1.3 Reef Experiments and Model Development

A two-week (25 March – 9 April 2014) field experiment was conducted on the intertidal reef platform on Tallon Island (16°24'S, 123°08'E) in the Sunday Island group near the southern limit of the Buccaneer Archipelago, where 17 hydrodynamic instruments recorded data continuously both on and off the reef platform. Ten RBR Virtuoso D|tide pressure sensors (denoted P1-P10) recorded water levels continuously at 1 Hz, at 4 locations offshore of the reef (P1-P4), thus located below the minimum tidal level during the experiment, as well as at 6

sites distributed on the reef (P5-P10) (Figure 3b). Five Nortek Vector acoustic Doppler velocimeters (sites V1-V5) were deployed on low profile tripods and measured velocities and pressure continuously at 2 Hz (Figure 3b); the Vector heads were mounted upward looking such that the velocities at a height 0.4 m above the bed were recorded. Finally, two 2 MHz Nortek Aquadopp profilers (sites A1-A2) were deployed on the reef and were mounted upward-looking flush to the bottom (Figure 3b). The A1 Aquadopp was operated in standard mode, and recorded the mean current profiles every 300 s using 0.1 m bins. The A2 Aquadopp was operated in high resolution (pulse coherent) mode with 0.03 m bins and sampled continuously at 1 Hz.

High resolution bathymetry was obtained by surveying the study area with a small boat at high tide using an echosounder integrated with a Real Time Kinetic / Global Navigation Satellite System (RTK-GNSS) to remove the effects of tide. The accuracy of the elevation measurements is estimated to be <0.05 m. However, the abundance of the large seagrass species (Enhalus acoroides) located within the back 500 m of the reef most likely contributed to some small positive bias (~0.2-0.3 m) in the measured elevations in this region. As the echosounder would likely detect the top of the seagrass canopy with leaf lengths ~0.3 m, this can explain the slight shallowing of the depth in Figure 3c that was not observed in the bottom-mounted pressure sensor data.

In addition, a numerical model based on the nonlinear shallow water equations using SWASH (Zijlema et al. 2011) was applied to investigate the hydrodynamics of the reef platform. While this code was designed to study the dynamics of wind waves, it is equally well suited for simulating the rapidly varied tidal flows in the present study. This was further used to develop a more general analytical model of tidal reef hydraulics to identify the fundamental relationships between key system parameters such as reef morphology, bottom roughness, and tidal properties. Details of the model approaches and methods are provided in Lowe et al. (2015).

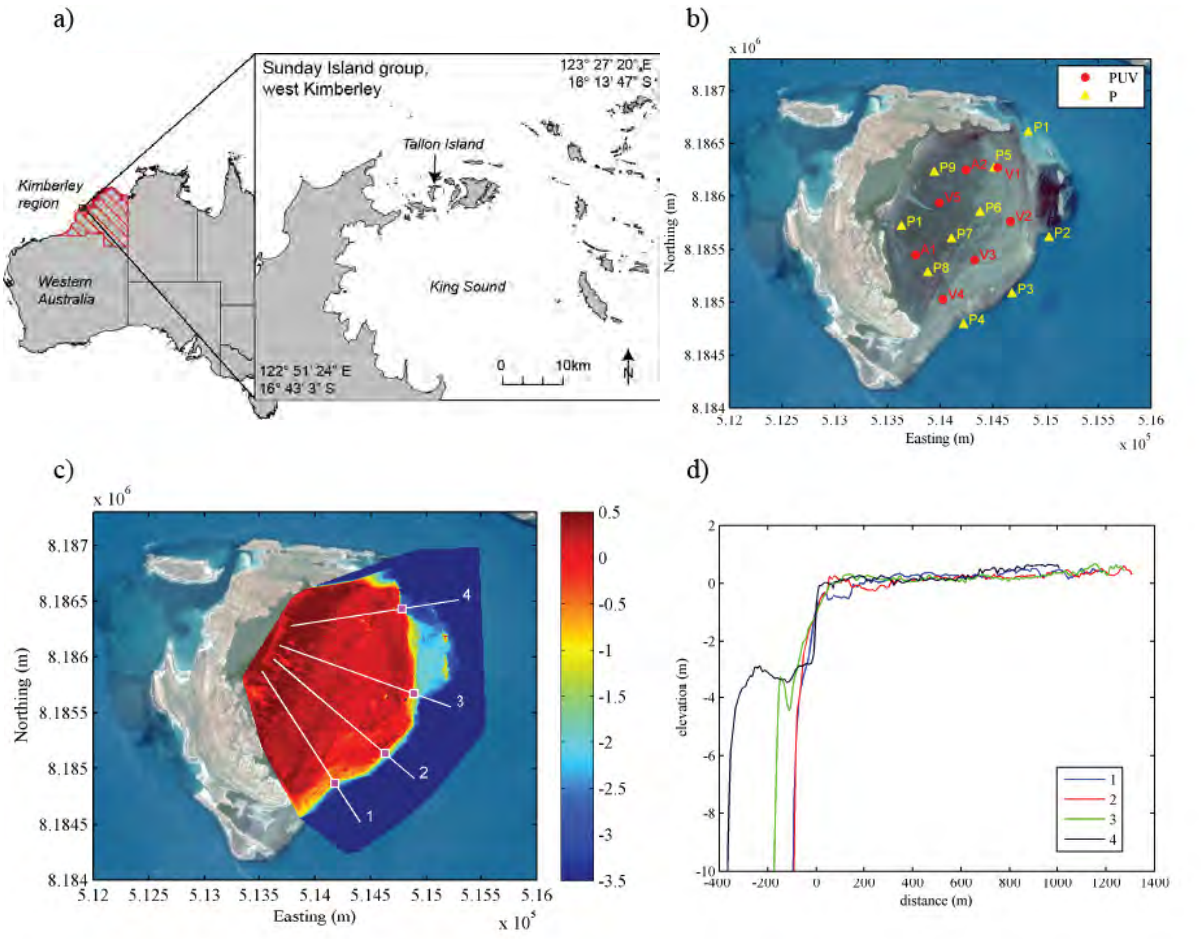

Figure 3 a) The study side on Tallon Island, in the Kimberley region of northwestern Australia. b) Aerial photograph of Tallon Island with the instrument sites superimposed. Red dots (PUV) sites denote acoustic Doppler velocimeters and profiles where both pressure and velocities were measured. Yellow triangles (P) denote locations where pressure sensors were deployed. c) Bathymetry relative to mean sea level (in m). The white lines denote four cross-reef transects, with the magenta squares highlighting the edge of the reef (x=0 m). d) Bathymetry profiles across the four transects in c), with the cross-reef distance relative to the reef edge.

2.1.4 Hydrodynamic ROMS model set-up

To describe the physical oceanographic processes, a numerical model based on ROMS was set-up covering the Camden Sound/Collier Bay region and tested against historical measurements in the region, and has been tested against mooring data and the field data from the two cruises to Camden Sound in October 2013 (dry season) and March 2014 (wet season). The details are described in Espinosa-Gayosso et al (2016). The model bathymetry and domain are shown in Figures 4 and 5. The grid scale varies, but is about 800 m at the offshore zone and 500 m close to the coast. Acquiring reliable bathymetry was challenging and model input data came from digitized navigation charts from CMap, Geoscience Australia data sets, topography from the USGS RSTM30 V6 database and data collected during the 2013 and 2014 trips. Resolution of model bathymetry is 30 sec or about 1 km. Tidal forcing was applied at the offshore boundary with tides taken from the TOPEX TPXO 7.2 Atlas. Wind, rain and heat forcing come from the ECMWF (ERA-Interim reanalysis). The dominant source of freshwater flow is from the Isdell River (Walcott Inlet) and this is estimated based on monthly average rainfall data and the baroclinic time step is 10 s.

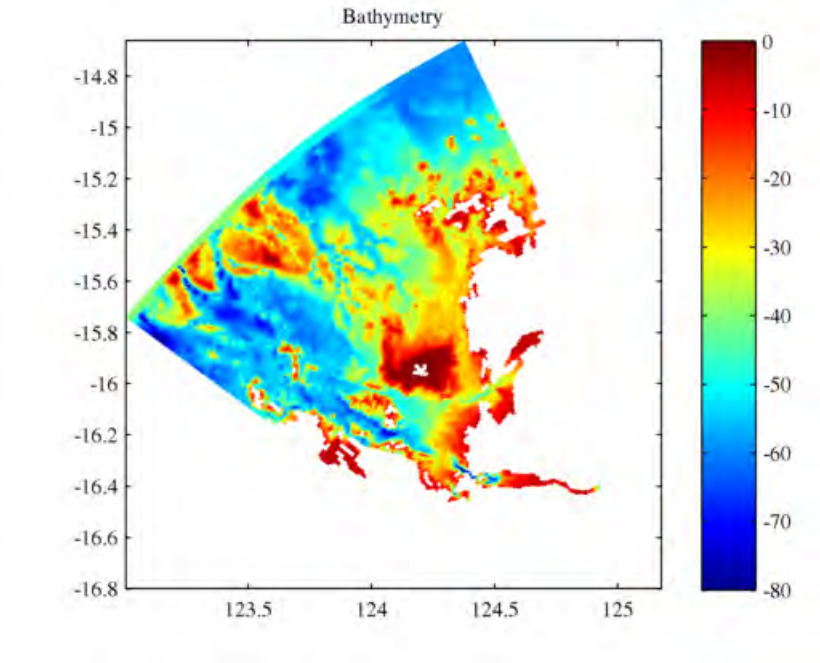

Figure 4 ROMS model domain and bathymetry.

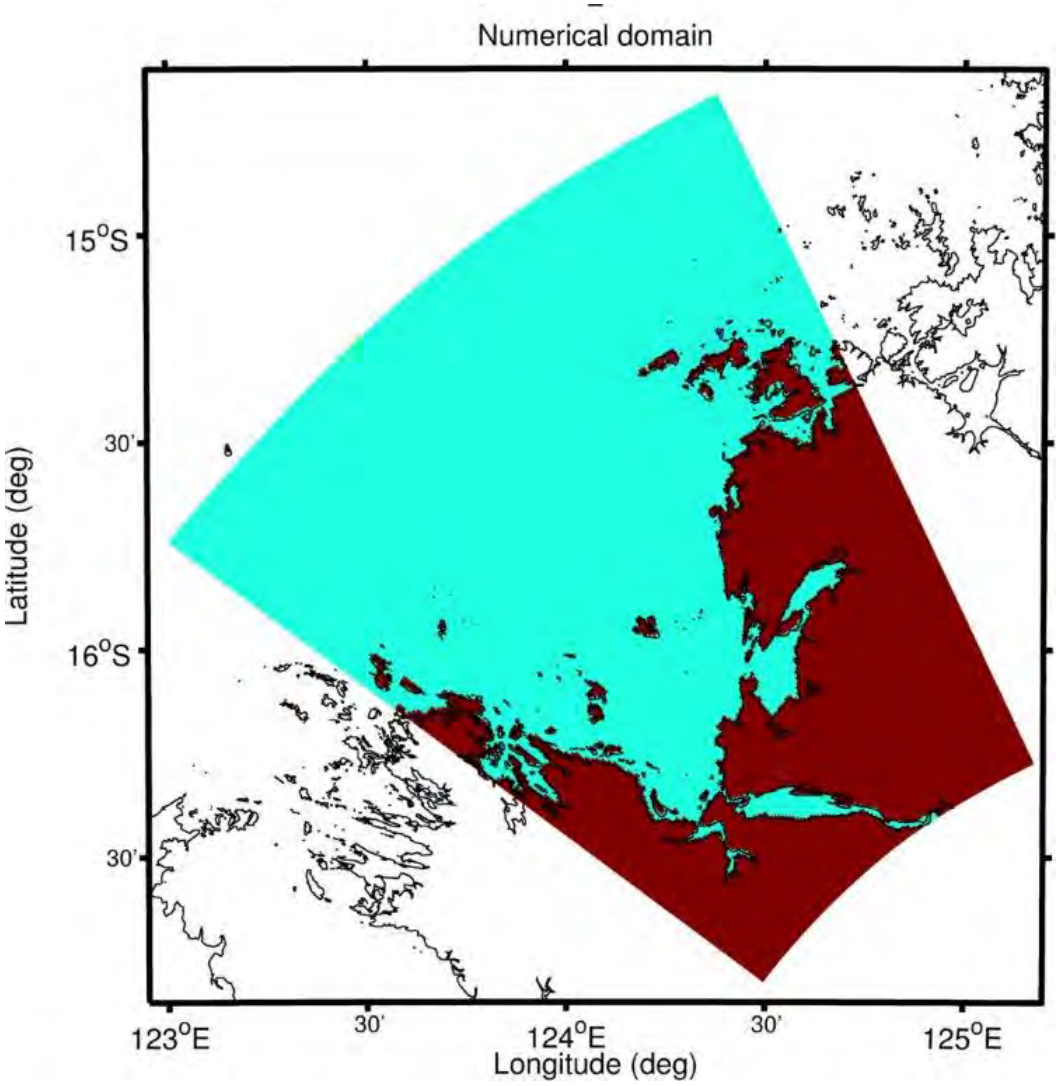

Figure 5 ROMS model domain for initial set-up

2.2 Data analysis

2.2.1 Calculation of residual currents

Tides are constantly fluctuating about the major/minor axes of the tidal ellipse in the macrotidal Kimberley environment. Residual velocities consider the net transport of particles in a system about this axis over timescales greater than one tidal cycle (Stacy 2001; Li 1997; Dyer 1997). To properly understand the net transport created by tidal forcing and buoyancy fluxes in the system, a time frame of one spring-neap tide or greater must be considered (Stacy 2001). Measurements of velocity taken at a single point are known as Eulerian velocity, (Eulerian residuals); measurements taken from following a particle as it changes position is Lagrangian velocity, (Lagrangian residuals) (Dyer 1997). Lagrangian is the most appropriate for demonstrating the mass transport of a velocity-affected system, like an estuary (Giddings 2014).

Giddings (2014) addresses the failure of common estuary/bay models in macrotidal environments by providing a method of depth normalization so that when averaging to gain residual flow of a system all points over time are comparable. The first step entails extrapolation of the z coordinates over a depth normalized coordinate system (σ) where σ = z/D, (z = vertical height, D= time varying water depth, z=D at surface and z=0 at bed) (Giddings 2014). This accounts for the large portions of data that would otherwise be outside the wetted area during low water level.

2.2.2 Tidal analysis

To separate the tidal constituents and their contribution to tidal energy; a tidal harmonic analysis was performed at all sites. The tidal analysis toolbox (t-tide) is a classical harmonic analysis for tide data a year in length or shorter that has been specifically designed for MATLAB and made freely available by its creator online (Pawlowicz et al 2002). An algorithm estimates all parameters in the t-tide analysis produces and provides confidence intervals for the accuracy for the phase for each constituent.

3 Results

3.1 Meteorological conditions

Rainfall data from the bureau of meteorology Mount Hart Station and Charnley River Stations is summarized in Figure 6.

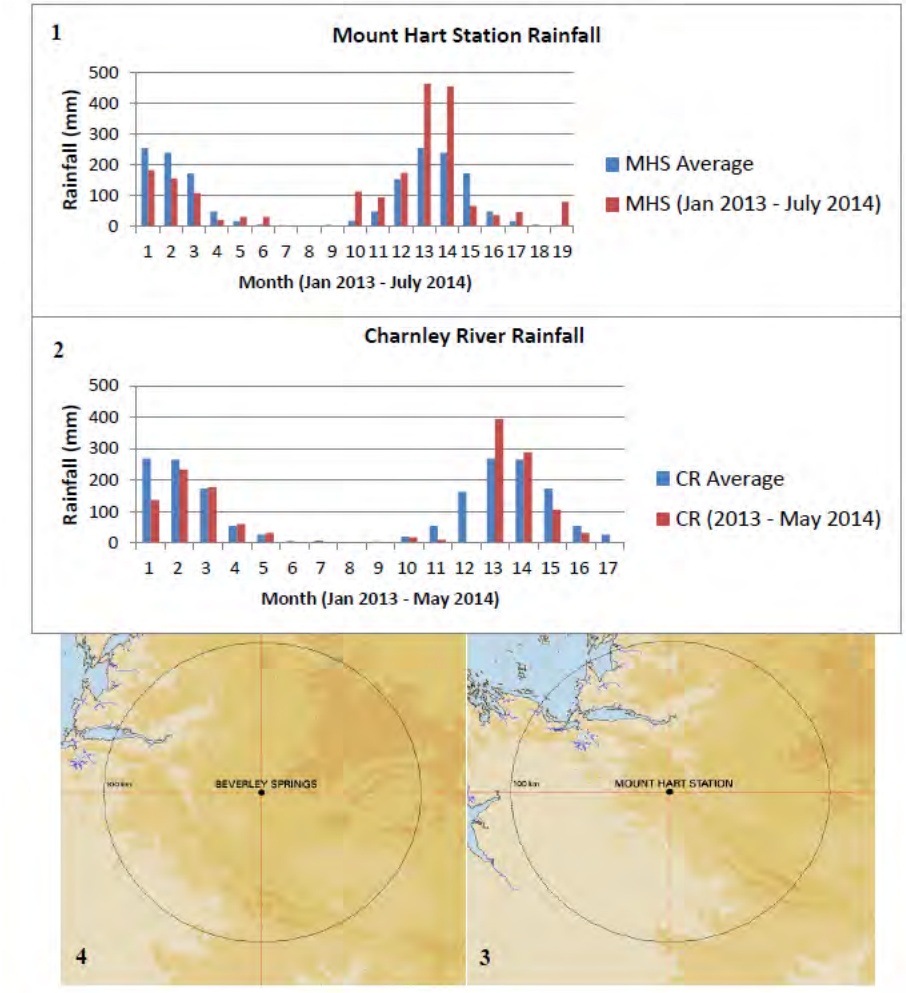

Figure 6 Meteorological data, 1) Mount Hart Station average monthly rainfall and 2013/14 rainfall comparison, (2) Charnley River average monthly rainfall and 2013/14 rainfall comparisons, (3) Location of Mount Hart and (4) Beverley Springs relative to Walcott Inlet.

3.2 Tidal analysis

The t-tide analysis allowed all major semi diurnal constituents to be separated and their respective amplitudes and phases calculated and compared. Table 1 lists the amplitude, surface elevation phase, stream wise velocity phase and phase difference for the three major constituents and the M4 at all four sites.

M2	Amplitude	SE Phase	Major Ellipse Velocity Phase	Phase Difference
WALCT	2.8662	132.96	230.09	97.13
WKINN	3.182	96.41	205.17	108.76
WKMID	1.4192	87.3	191.39	104.09
WKOFF	2.0796	83.83	192.99	109.16
S2	Amplitude	SE Phase	Major Ellipse Velocity Phase	Phase Difference
WALCT	1.3328	198.37	125	73.37
WKINN	1.8886	160.43	90.82	69.61
WKMID	0.833	150.2	76.62	73.58
WKOFF	1.2247	144.58	75.07	69.51
N2	Amplitude	SE Phase	Major Ellipse Velocity Phase	Phase Difference
WALCT	0.4203	126.07	52.47	73.6
WKINN	0.5641	69.6	357.85	288.25
WKMID	0.2481	62.76	344.88	282.12
WKOFF	0.3835	60.57	349.42	288.85
M4	Amplitude	SE Phase	Major Ellipse Velocity Phase	Phase Difference
WALCT	0.0398	137.32	80.97	56.35
WKINN	0.5641	95.45	216.98	121.53
WKMID	0.2481	57.25	183.35	126.1
WKOFF	0.3835	67.38	14.48	52.9

Table 1: Phase and amplitude of the major tidal constituents (M2, S2, N2 and M4) at the four mooring sites shown in Figure 1. The sites are Walcott Inlet (WALCT), Walcott/Inner shelf (WKIN), Walcott/Mid shelf (WKMID) and Walcott/Outer shelf (WKOUT).

3.3 Mass transport residuals

The mass transport residuals (MTR) were calculated and plotted for each site. As stated in section **Error! Reference source not found.**, the MTR estimation is a combination of the Eulerian velocity residual and the Stokes drift transport residual, this can be seen in Figure 7 where the two provide the overall shape of the mass transport, in red. This has been provided to show a visual representation of how the MTR was calculated and how all components act within the water column

.

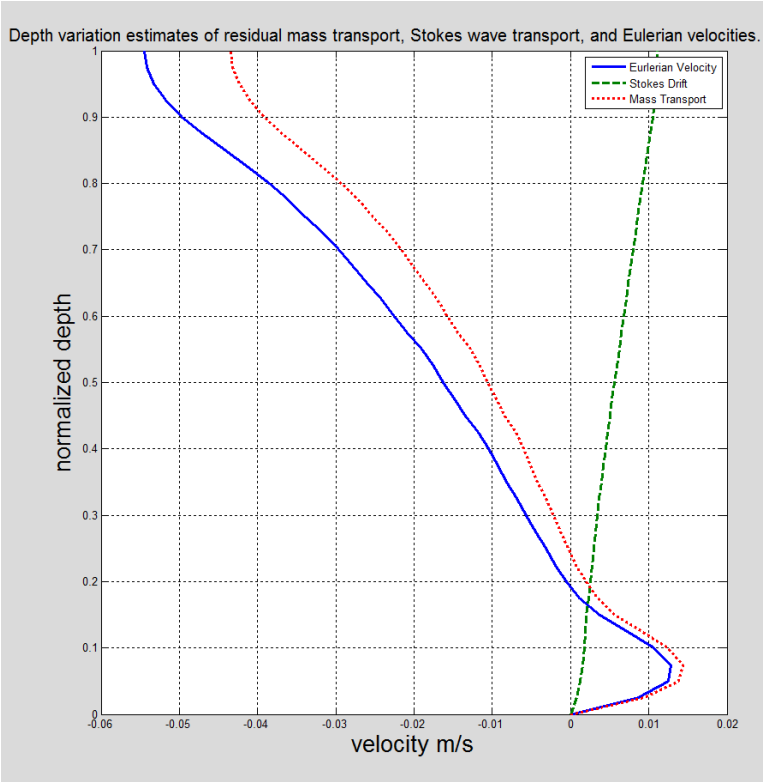

Figure 7 Eulerian and wave transport estimates producing the mass transport estimate for Stream Wise flow at WALCT inlet.

At site WKINN (Figure 1 and Table 1) during a spring-neap cycle within a zero rainfall period (DRY) there is close to zero residual mass transport for the entire water column, never reaching any greater than |0.01| m/s in either direction (figure 8). During the low rainfall spring-neap period (MID) there is increased variance in the flow residuals with the maximum flow reaching -0.06 m s+-1 at the surface, however the net flow for the bottom 60% remains around zero.

The residual mass transport increased significantly during the spring-neap cycle at maximum rainfall (WET) with an upstream flow near the seabed and a downstream flow at the surface. The bottom 36.5% of the water column produces upstream residuals with a maximum reached of 0.04 ms^{-1}. Beyond this point the residual flow is downstream, reaching a maximum at the surface of -0.11 ms^{-1}.

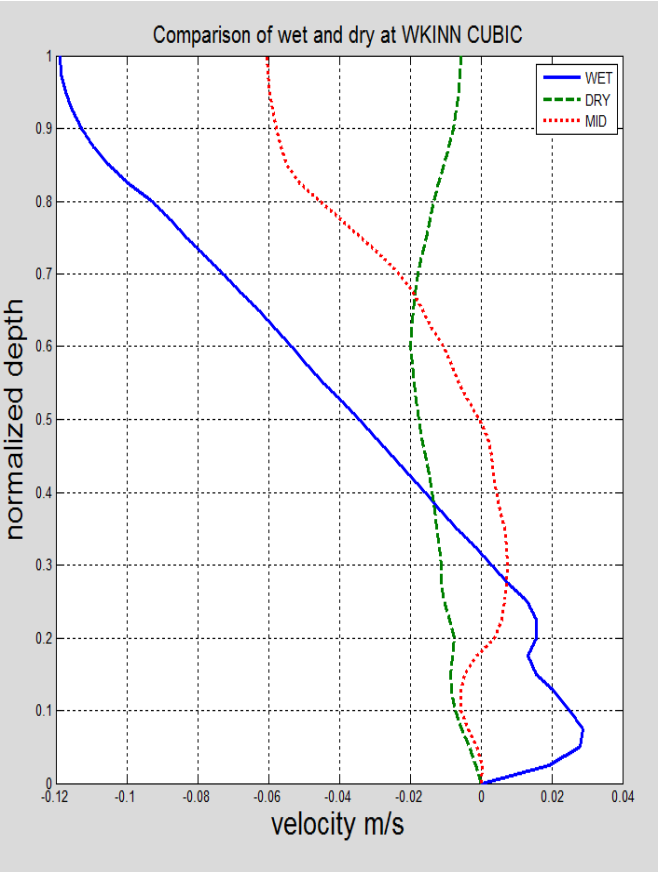

Figure 8 Residual currents at WKINN for 3 different rainfall conditions

3.4 Moored salinity data

The surface and near bottom salinity were similar when the rainfall was low (Figure 9). As the rainfall increased the overall salinity dropped and the water column became salinity stratified.

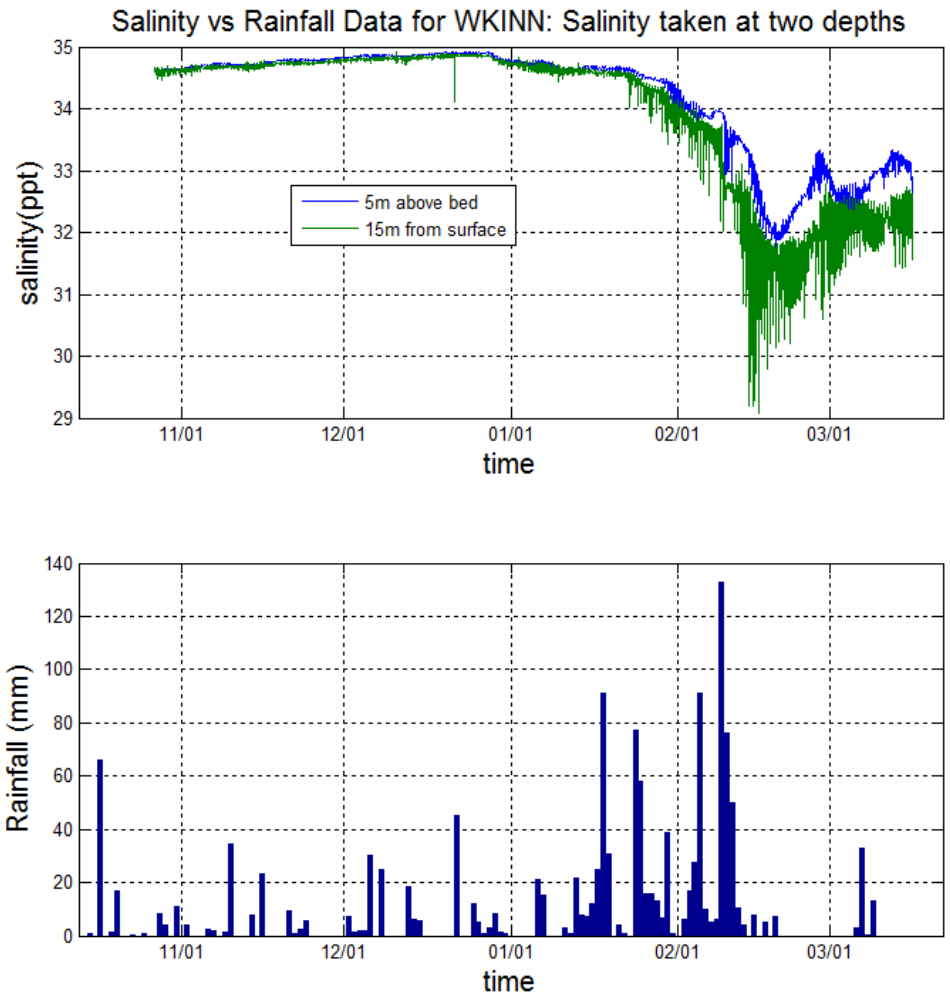

Figure 9 Salinity data from site WKINN and rainfall data from Mount Hart

Following the rain the decrease in salinity was also seen at the site furthest from Walcott Inlet (WKOFF), albeit a much smaller change (Figure 10). The water temperature generally increased over the sample period as expected during the hot, wet season.

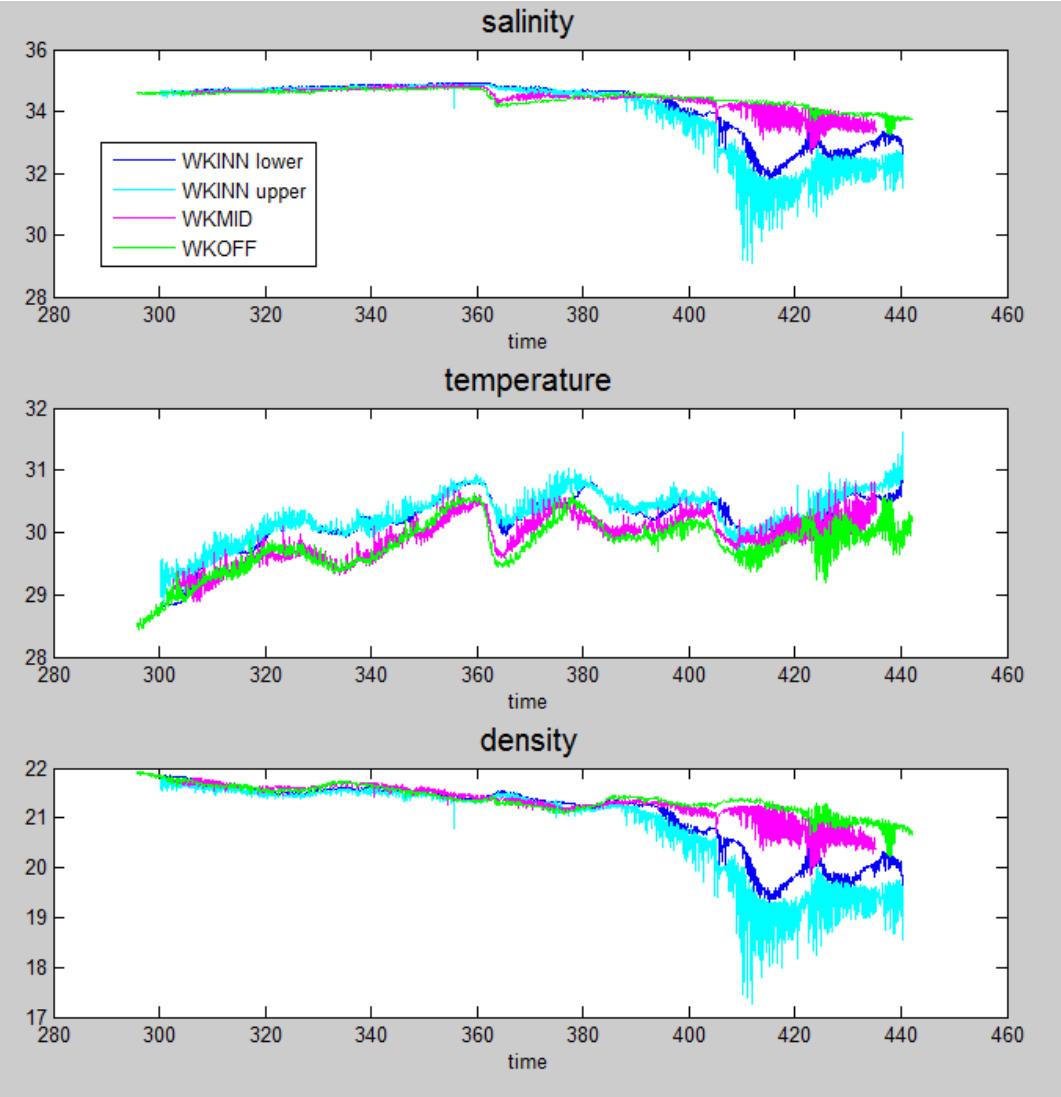

Figure 10 (a) Salinity, (b) temperature, (c) density at sites WKINN, WKMID and WKOFF.

3.5 Reef hydrodynamic processes

Figure 11a shows the water level η (relative to the MSL offshore) over the two-week study period, at representative sites offshore (P1) and near the back of the reef (P9). Tidal variations offshore reached a spring maximum of ~8 m offshore (P1) during the middle of the study and a neap minimum of ~3 m around the beginning and end of the study. In contrast, tidal variations on the reef (P9) were substantially reduced, varying between ~3 m during spring tide to only ~1.5 m during neap tide.

A cross-comparison of the water levels between the various sites is shown for a single representative spring tidal cycle in Figure 11b,c; however, the general trends were similar during the other tidal cycles, differing only in magnitude. During the flood phases of the tide ($-2 < t < +2$) reef water levels closely followed the quasi-sinusoidal changes in offshore water levels; however, after $t \gtrsim 2$ hrs the water drained much slower off the reef, resulting in a highly asymmetric tide (Figure 11b). For $t \approx$ 2-4 hrs the reef water level fell at ~1.0 m h^{-1} versus ~1.8 m h^{-1} offshore; however, later (after t=5 hr) the water level fell at a rate of only ~0.1 m h^{-1}. During the flooding tide, there was a 1 hr period where the offshore water level was up to 1 m higher than on the reef due to the delay in the tide propagating across the shallow and rough reef. Over this period the water level rose much more rapidly on the reef until it reached an equilibrium with the offshore water level ~3 hr before the peak high tide.

Figure 11c highlights differences between the offshore water level time series at sites along the reef (P1-P4). For all of these sites, the water levels were in close agreement during the flood phase of the tide. However, during

the ebb phase the water levels are slightly lagged from P1 to P4. This likely reflects the effect of island blocking, with the sites from P1 to P4 being increasingly located upstream of the island relative to the ebb direction of the tide exiting King Sound. This leads to a modest along-reef water level gradient when the offshore water levels are above the reef height during the start of the ebb (Figure 11c).

To investigate how the tidal circulation varies on the reef during each tidal cycle, the velocity records were conditionally sampled based on the phase of the offshore tide (P1) and then phase-averaged over all of the individual tidal cycles (Figure 12). At all sites there is a substantial asymmetry between the ebb and flood currents, both in magnitude and duration. During the ebb phase, the maximum flow speed tends to peak 2-3 hours after peak high tide (Figure 12a,b) but this lag time increases slightly from north to south along the reef (i.e., from V1 to V4). The ebb flow also tends to be stronger along northern parts of the reef edge (i.e., V1 and V2 versus V3 and V4). Roughly 4 hours after the peak high tide, the water drains slowly off the reef with speeds <0.2 m s^{-1}.

During the flood phase, the maximum flow occurs within 1 hour after the water level rises above the reef edge (i.e., at t≈10 hrs.). The magnitude of the peak flood flow relative to the peak ebb flow varies among the sites, and can be either slightly weaker or stronger, except at V1 where currents generated by the flood tide were ~40% weaker. Most notably, the duration of the flood is much shorter than the ebb, lasting only 1-2 hours.

Tidally averaged current vector fields at different phases of the tide are shown in Figure 13 (note that a different vector scaling is used for different phases of the tide to highlight the tidal velocities even when the flows are relatively small). During the initial two hours after peak high tide, coinciding with the period where the offshore-directed flow also accelerates (figure 13b), the flow tends to be northwestward throughout the reef with most of the discharge occurring on the northern section (Figure 14b-d). This northward flow is consistent with the along-reef component of the water level gradient that is present during the initial ebbing of the tide. After t≈2 hrs., when offshore water levels have dropped below the reef rim, the along-reef pressure disappears on the reef platform despite being present offshore, and the flow generally drains more uniformly off the reef (i.e. the flow vectors become directed roughly normal to the orientation of the reef edge). This slow draining ebb period lasts until t≈10 hrs. when the tide floods the reef platform once again, and the flow becomes uniformly oriented in the cross-reef direction along the entire reef due to the absence of any substantial along-reef pressure gradient.

The asymmetries in the magnitude, duration and spatial pattern of the tidal flows generate residual flows every tidal cycle. To quantify this residual transport, for each site we compute the time-averaged discharge vector $\langle \vec{q} \rangle$. Figure 14 reveals a residual discharge of $\left| \langle \vec{q} \rangle \right|$=0.1-0.2 $m^2 s^{-1}$ towards the northeast, leading to a net onshore component of the residual flow along the southern edge of the reef and an offshore component of the flow along the northern edge. This net northward residual flow primarily arises from the northward flow that occurs on the reef for a relatively short (~2 hr) period directly after peak high tide (i.e., Figure 11b-d). This corresponds to ~10-20% of the average maximum flow q_{max} observed over the tidal cycle at each site.

The detailed numerical model developed using SWASH was able to accurately describe the tidal hydraulics on Tallon reef, including the large ebb-flood asymmetries in both water level and currents (Figure 15). Details of the model configuration and application are described in Lowe et al. (2015). The model importantly reveals the dominant momentum balances that are established on the reef, and how flow resistance due to reef bottom roughness restricts water draining off the reef and allows it to remain submerged over a full tidal cycle despite the offshore mean water level falling far below the reef elevation (by several meters). These dynamics are critical to explaining how productive reef communities are able to survive and thrive in this macrotidal environment.

While the focus of the field study was on the dynamics of Tallon reef as a case study, Lowe et al. (2015) also develops a more general framework for predicting the hydrodynamics of intertidal reef platforms (see that paper for details). In particular, the analytical model developed in that study reveals how tidal draining of the water

level on reef platforms decays as $\left(t/\Phi_f T_d\right)^{-1}$, where T_d is a reef draining time-scale that depends on properties of the reef morphology and tidal range and Φ_f is a dimensionless friction parameter that depends on the reef bottom roughness characteristics (refer to that detailed descriptions of these parameters). The model was able to accurately reproduce the water depth decay for a wide range of physically probable bottom drag coefficient C_d and reef width L_r values (Figure 16). This provides physical insight into how very productive reef ecosystems living within the intertidal zone of reefs in the Kimberley high above the offshore low tide elevation can remain submerged (and hence survive) over a full tidal cycle.

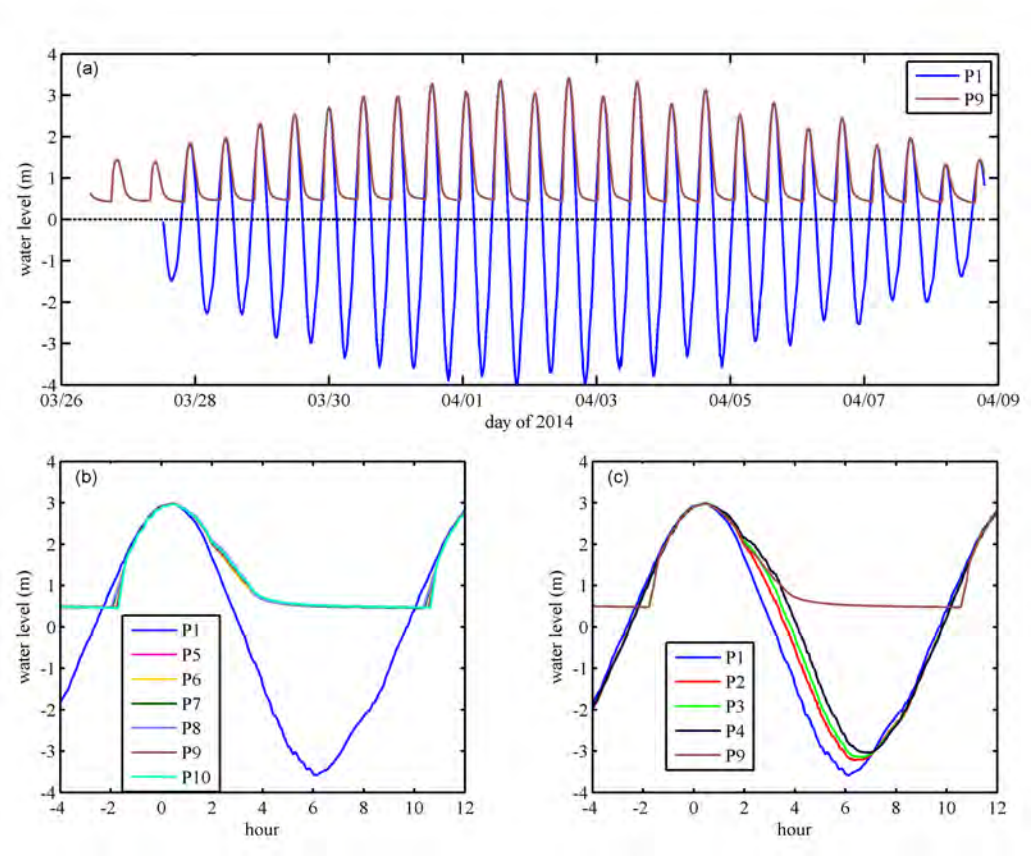

Figure 11 Water level variability. a) Water level variations at a representative site offshore (P1) and on the reef (P9) for the entire experiment. For a single tidal cycle on 2 Apr, b) the water levels measured at all pressure sensor sites on the reef (P6-P10) relative to offshore (P1), and c) measured at all offshore sites (P1-P4) relative to on the reef (P9).

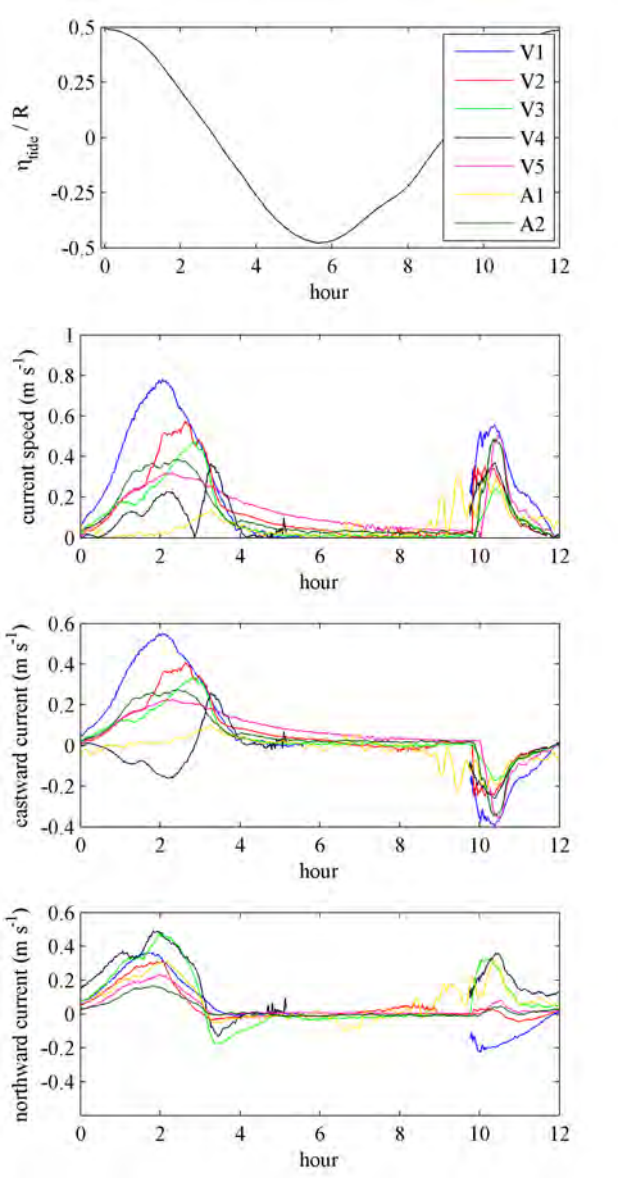

Figure 12 Tidal current variability on the reef. a) The reference offshore tidal elevation at P1. Tidal phase-averaged b) current speed, and c) eastward and d) northward current vector components.

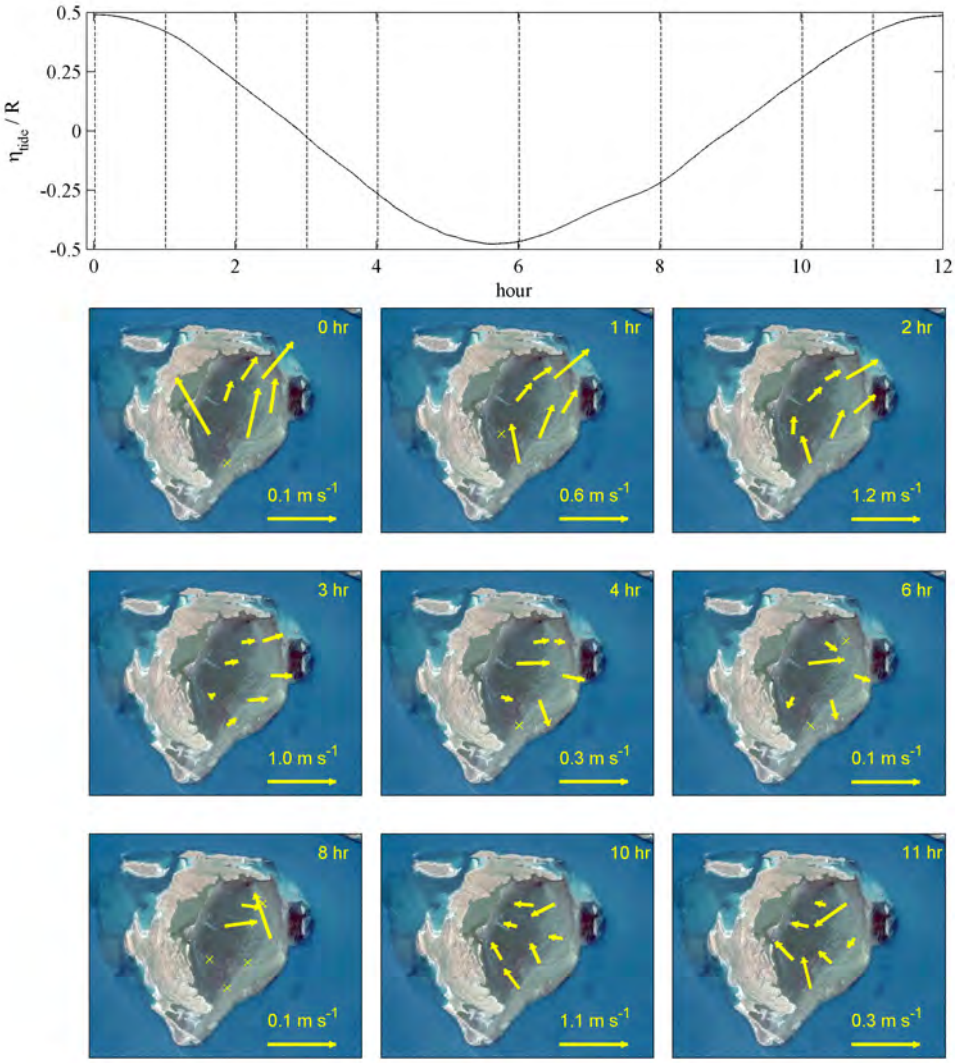

Figure 73 Tidal current vector fields on the reef at select phases of the tide. a) The tidal phased-average reference offshore water level at P1, normalized by the mean tidal range. Vertical dotted lines denote the select phases of the tide plotted in b)-j). Tidal phase-averaged current vectors at select phases of the tide, referenced to time of peak high tide; b) 0 hr; c) 1 hr; d) 2 hr; e) 3 hr; f) 4 hr; g) 6 hr; h) 8 hr; i) 10 hr; j) 11 hr. Note that the current vectors are scaled substantially among figures to emphasize the current patterns when the flow is relatively weak (refer to the reference current vector for scaling differences).

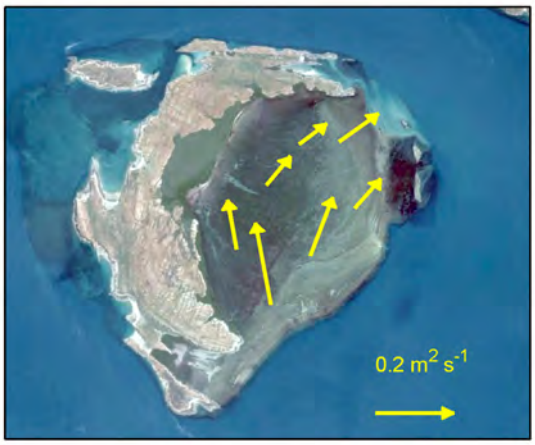

Figure 84 Residual discharge vectors computed for the duration of the experiment.

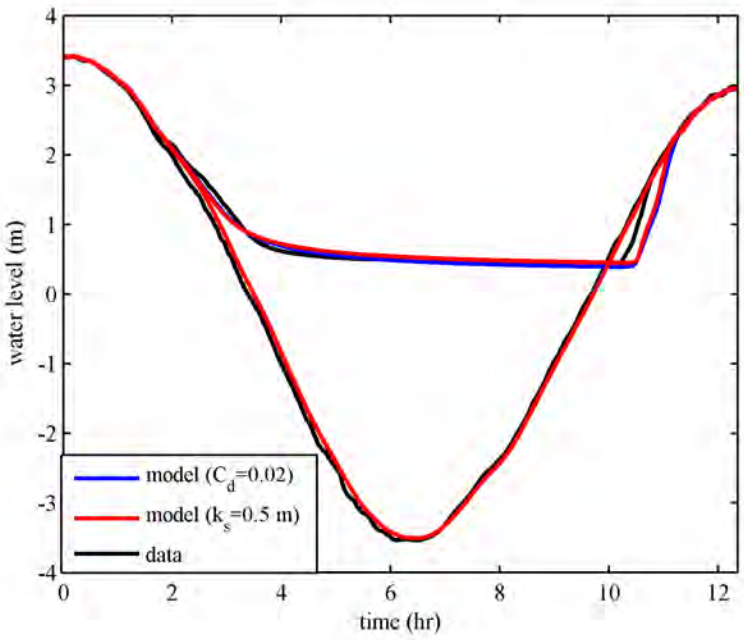

Figure 95. Comparison of the modelled versus observed water levels both on and the off reef platform, showing results for a tidal cycle on 2 Apr during the spring phase of the tide. Model results are shown using both a constant drag coefficient formulation with Cd = 0.02 and a logarithmic formulation (Eq. (6)) using ks = 0.5 m. For the water level on the reef, the rms error of the prediction is 0.06 m and the skill is 0.99 for both drag formulations.

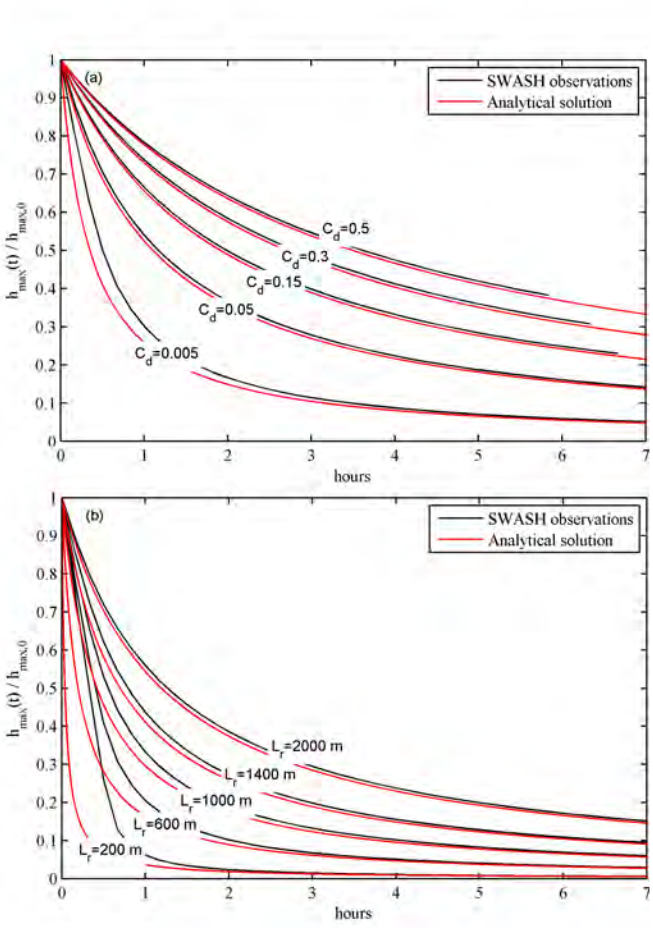

Figure 106. Effect of varying bottom drag coefficient C_d and reef width L_r on the reef water depth decay and comparison between the SWASH and analytical model results. a) Effect of varying C_d with the reef width held constant at L_r = 1400 m. b) Effect of varying L_r (in meters) with the drag coefficient held constant at C_d = 0.02. For consistency, in all cases the analytical model comparison commences when $h_{\max,0}$ = 1 m.

3.6 ROMS numerical modelling

Espinosa-Gayosso et al (2016) describe the results of the numerical modelling. Figure 17 a, b, c shows inter-comparison of tidal elevation and depth-averaged or barotropic velocity of the model predictions and the field measurements from moorings at the outer bay (45m local depth), mid bay (55m local depth) and inner bay (35m local depth), for both the wet season periods. As can be seen both sea-surface height and barotropic velocity are in excellent agreement between the two over the full spring-neap tidal cycle.

a)

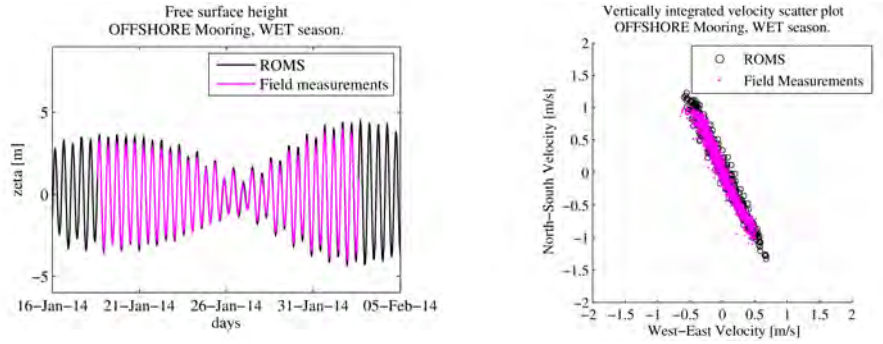

b)

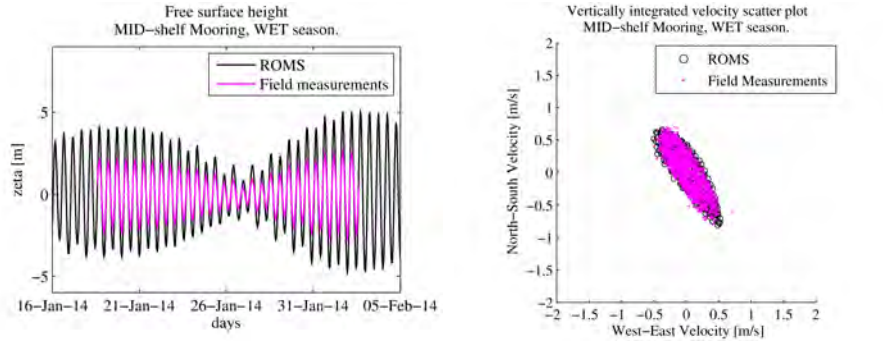

c)

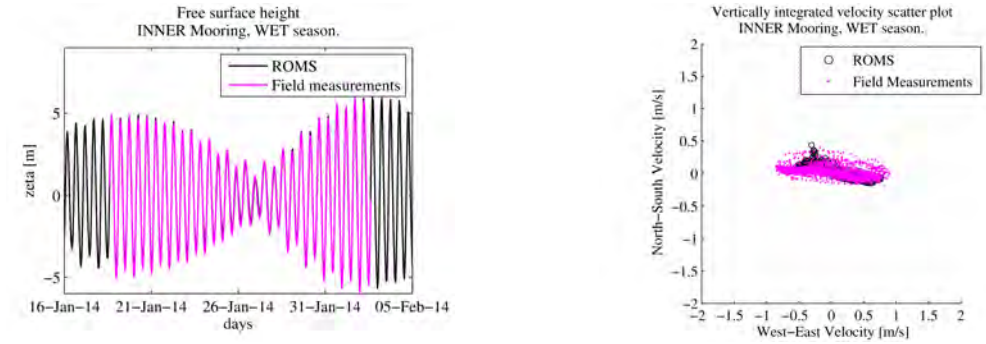

Figure 117 Comparisons ROMS predicted sea-surface height and depth-averaged velocity with moorings for a) offshore mooring at 45m, b) mid-shelf mooring at 55m and c) inner moorings at 35m.

In Figure 18 we show an example of the instantaneous and tidally averaged velocity profiles over the depth at the inner mooring site, over three different periods in the annual cycle, again showing good agreement between model and observation of the through-the-water column profiles.

a)

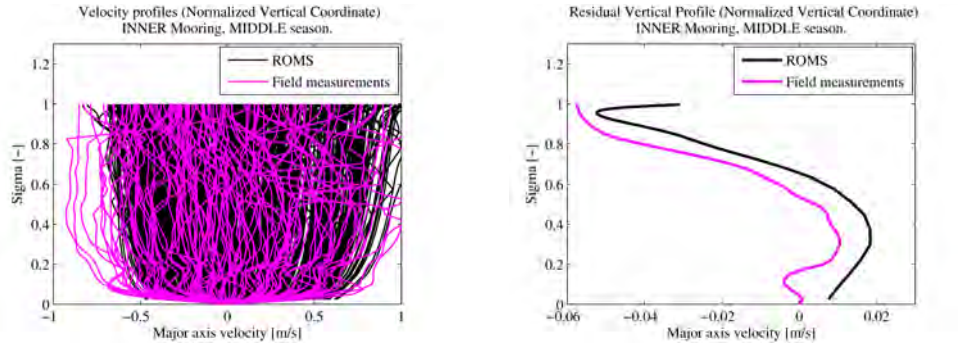

b)

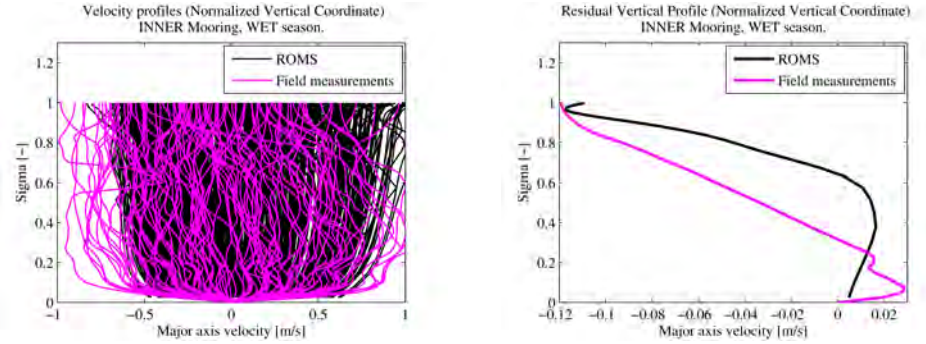

c)

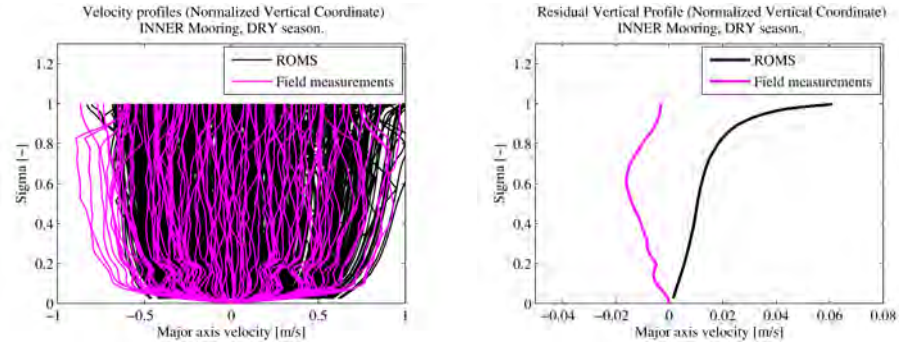

Figure 128 Comparisons ROMS predicted and measured velocity with moorings for inner moorings at 35m at a) middle season b) wet season c) dry season

The residual circulation, or circulation that can be seen on time scales longer than a tidal period, can be calculated in two frameworks: an Eulerian analysis, based on the velocity time series at fixed locations; and a Lagrangian analysis, based on the displacement of particles following the flow field. The Eulerian-based procedure is based on the velocities at the centre of the horizontal grid cells. The Lagrangian procedure considers the residual velocity as the distance travelled by a particle during a complete tidal cycle, divided by the tidal period, and is sensitive to the exact phase of the tidal cycle when the analysis is initiated. The results of both methods are

shown in Figure 19 (note that the colour scale for the residual velocity magnitude in the Figure is logarithmic.). While the two methods are not identical, they yield similar results (see Espinosa-Gayosso et al (2016)).

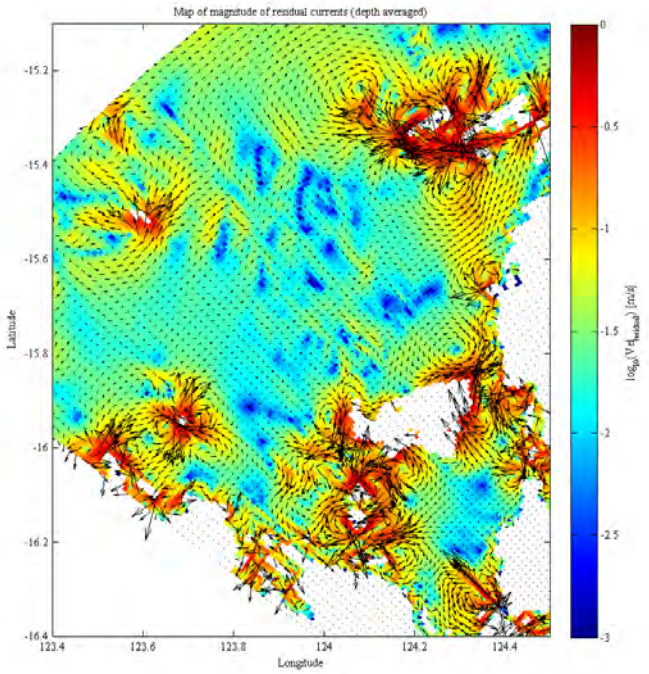

(a)

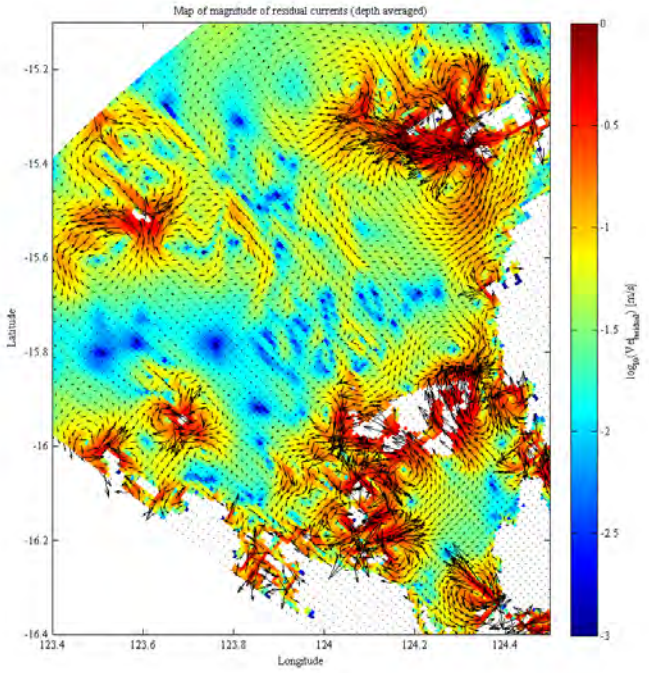

(b)

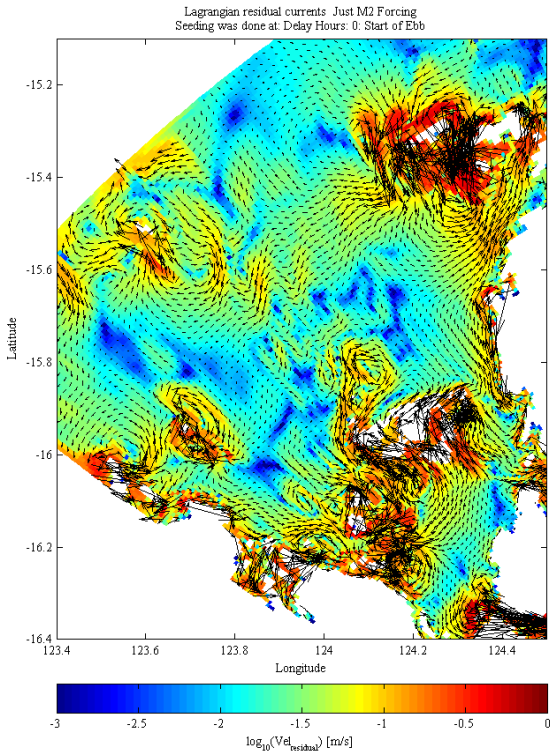

(c)

Figure 19 Residual fields for a simulation forced by dominant M2 tide (a) Eulerian residual field. (b) Lagrangian residual field with particles liberated at the beginning of ebb (c) Lagrangian residual field with particles liberated at the beginning of flood. (colour scale ranges from 1 mm/s (dark blue) to 1 m/s (dark red)).

From both methods, it can be seen that residual velocities vary strongly with between highs of 1m/s in channels to lows of 1cm/s in open areas. A large low residual velocity region exists in the interior of the bay near (16.2°S, 124.3°E) and the other one at the outer area near (15.6°S, 124°E). Another consistent feature is the presence of a current directed towards the Bonaparte Archipelago (15.5°S, 124.4°E) which we term the 'Bonaparte' current here. The very high residual velocities are in channels and large reef areas. For example, the inward-directed jet at the Caesar Channel (16.2°S, 124.2°E) is consistent in all the residual fields. This inward jet is followed by a recirculation loop that shows water flowing inwards through Caesar Channel and outwards on top of the western part of Montgomery Reef. The footprint of the jet flowing northward from the interior of the Walcott Inlet estuary (16.35°S, 124.35°E) also appears consistently in all the residual fields. In broad terms this suggests a large-scale anti-clockwise residual circulation in the Bay as a whole. These features are discussed below in the context of the overall flushing.

To demonstrate the links between the circulation and the flushing, in Figures 20 and 21 we show a model output from simulation during the wet season, over a three month period with freshwater input determined from rainfall through the Isdell River, and maximum flow rate being 800 m^3/s. Tracer model studies show that water predominantly enters Collier Bay from the Northwest side and exits to the northeast side (i.e., east of Montgomery Island) consistent with the idea of a general underlying anticlockwise circulation. By the end of the wet season, freshwater input through Walcott Inlet has been considerably diluted with seawater, but has penetrated some 50 km offshore and with a general preferential location along the eastern side of Collier Bay.

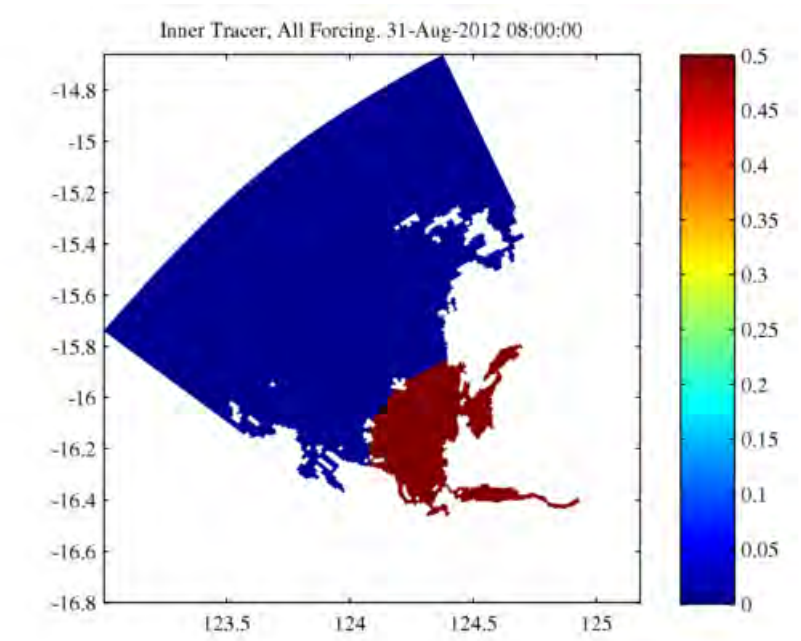

Figure 20 Sample ROMS prediction of the extent of freshwater influence in Collier Bay during the wet season showing initial conditions for passive scalar distribution. The colour scale range is 0 to 0.5 in order to enhance the resolution in Figure 21 below.

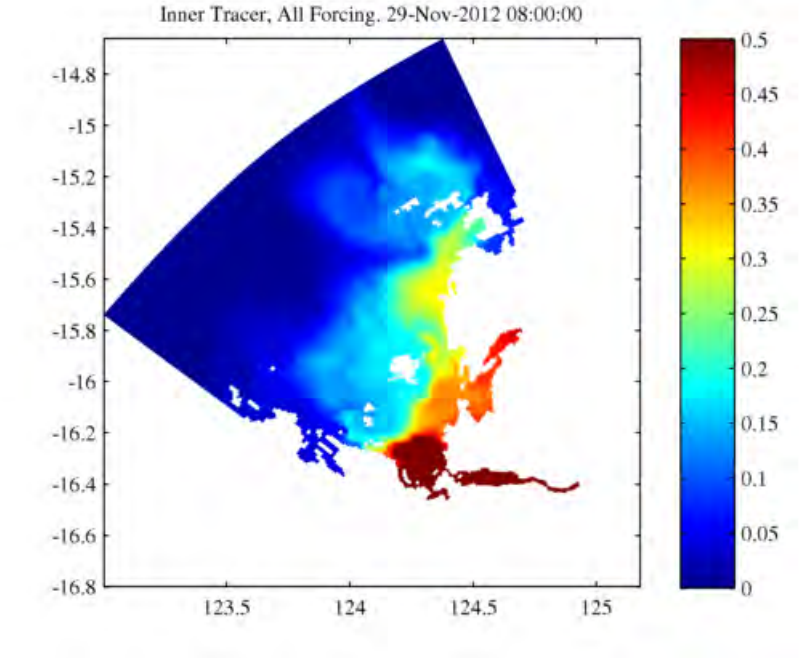

Figure 21 Final conditions for passive scalar distribution, 3 months after conditions shown in Figure 20.

In summary, the ROMS model has been set-up with tide, wind, heat and freshwater input forcing. The model is in excellent agreement with field observations. The model runs demonstrate the stability of the model and in

the macrotidal shallow water environment of the Kimberley this is a significant accomplishment. Significant progress has been made on quantifying the net circulation and exchange processes within the region. With inflow data obtained from project 2.2.6, the influence of the freshwater inflow has been studied by undertaking yearlong simulations.

3.7 Exchange fluxes

As shown above, in broad terms there is a slow anti-clockwise residual circulation. Due to the flow restrictions of the reef/island channels, highly energetic jets are locally generated at each tidal cycle, reversing direction every tidal cycle, and pumping water masses and material both in and out of the coastal region. This tidal pumping is the underlying mechanism that drives the residual circulations that are spatially very complex, reflecting the complexity of the underlying topography/bathymetry. With the tidal pumping is the underlying mechanism, an important question is the estimates of the overall flushing of the system, and this can be determined from both an Eulerian and Lagrangian perspective.

To accomplish this we consider the bay-scale control volume shown in Figure 22a with a near-shore coastal control volume with an open outer boundary. This boundary runs from the western to eastern coasts, and can be sub-divided into several sections as shown. A major section is Caesar Channel to the west, with a west sub-section (CCw) and an east sub-section (CCe) reflecting the distinct behavior of the Eulerian-based fluxes in the area. Vinney Passage is also a major section and this was also divided into two sections, denoted VPw and VPe, for the same reason. The shallow regions of Montgomery Reef were also considered as separate section and divided into a number of sub-sections as shown (MRw and MRe).

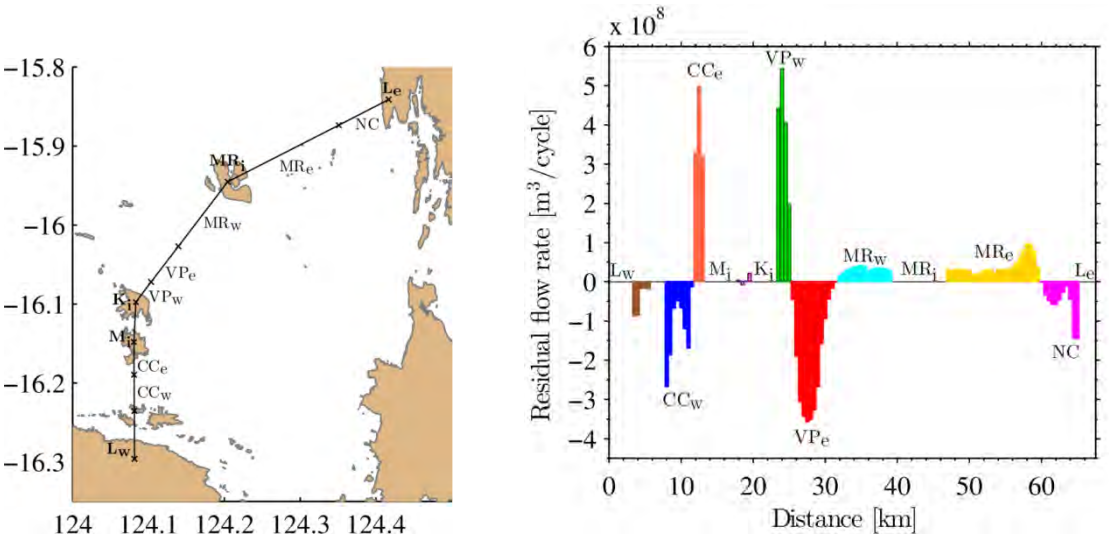

(a) (b)

Figure 22 (a) Map of the boundary defined across the several channels that connect the interior of Collier bay with the open ocean. (b) Histogram of the Eulerian-based M2-forced residual flux along the boundary (positive values indicate residual flux towards the open ocean). Each histogram bin corresponds to a sector of 500 m wide and blank spaces correspond to land or islands. Different colours are used for the different sections depending on their residual behaviour. Important sections have been labelled as: Land west (Lw), Caesar Channel west (CCw), Caesar Channel east (CCe), Melomy island (Mi), Kingfisher island (Ki), Vinney Passage west (VPw), Vinney Passage east (VPe), Montgomery Reef west (MRw), Montgomery Reef island (MRi), Montgomery Reef east (MRe), North channel (NC), Land east (Le).

In Figure 22b we show the results of the Eulerian flux analysis with net fluxes across the boundary shown in the Figure 22a for each 500m long section. The flux is complex with both outflow (positive values) and inflow (negative values) along the boundary. In terms of overall flux, the two dominant contributors are Vinney Passage

with the highest outgoing (positive) and incoming (negative) flow rates, and Caesar Channel with the second highest values.

A Lagrangian flux estimate can also be obtained from following particles as they cross the boundaries and the results are shown in Figure 23a,b, c, d, e & f. In order to track the particles visually, we have marked the particles with the same colours as for the Eulerian-based residual fluxes. Particles that crossed through a specific section were marked with the corresponding colour of that section. Therefore, particles crossing in or out through the North Channel (NC) were marked with magenta, those crossing in or out through the eastern part of Montgomery Reef (MRe) were marked with yellow, for example. Every time a particle crossed the boundary it was marked with the corresponding colour of that last crossing, even if already marked before due to a previous crossing. Therefore, particles always show the colour of their most recent crossing. Grey particles are those that have never crossed the boundary. Particles were released at the ebb tide condition at the beginning of flood and at the mid-depth layer. All the snapshots in Figure 23 correspond to a condition of slack flow at the end of flood (Figures 23 a, b, c) or at the end of ebb (Figures 23 d, e, f). This helps to identify the extent of local jet influence and the tidal pumping or trapping that occurs on each side of the boundary after every cycle.

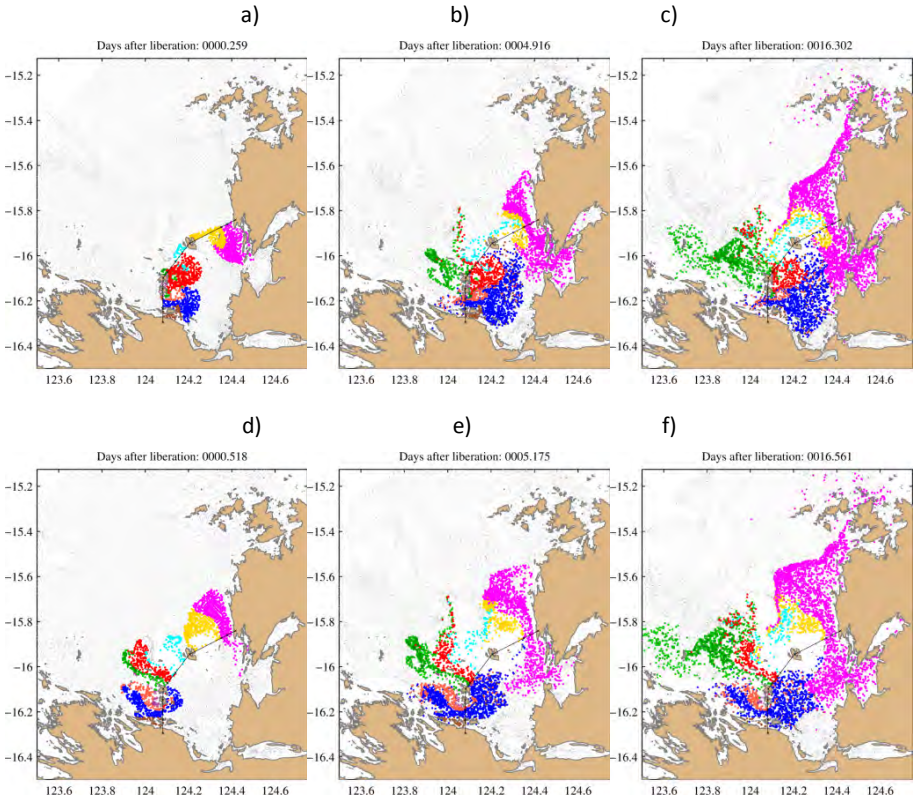

Figure 23 Series of snapshots of Lagrangian particles showing the sections where they have crossed the boundary (black line) for the M2-forced simulation. All snapshots in the first line (a,b,c) are for a slack condition at the end of flood for the (a:) 1st cycle, (b) 10th cycle, (c) 32nd cycle. All the snapshots in the second line (d,e,f) are for a slack condition at the end of ebb for the (d)1st cycle, (e) 10th cycle and (f) 32nd cycle. After any particle crossed a specific section, it was marked with the colour corresponding to that. Coloured particles always show the colour of their last crossing. Grey particles are those which have not crossed the boundary yet.

The maximum extent of the incoming channel jets can be identified from the snapshots in Figures 23a. Large 'mushroom-like' patches formed by particles coming from the North Channel (magenta), Vinney Passage east (red) and Caesar Channel west (blue) show the effect and the extent of these jets, and all jets reach approximately the same excursion in across the boundary (around 18 km). Similarly, the maximum outward excursion of the

particles towards the open ocean can be observed carried by the jets formed at the North Channel (magenta) and Vinney Passage (red & green) and show the large offshore excursion (Figure 23d) (around 23 km). The end of ebb condition (Figure 23 d) shows that particles coming from Caesar Channel (blue) and North Channel (magenta) are effectively pumped into the bay at every cycle. The cumulative effect after multiple cycles is clear in Figures 23de,f. There is no cumulative major inwards pumping of particles through Vinney Passage or on top of Montgomery Reef (Figures 24 e,f). The cumulative effect of net particle export over a number of cycles can be seen in the series of snapshots at the end of flood in Figures 24a,b. As also seen in Figure 24, after multiple tidal cycles, particles flowing out through the North Channel (magenta) and Vinney Passage west (green) are identified as the major export routes for particles.

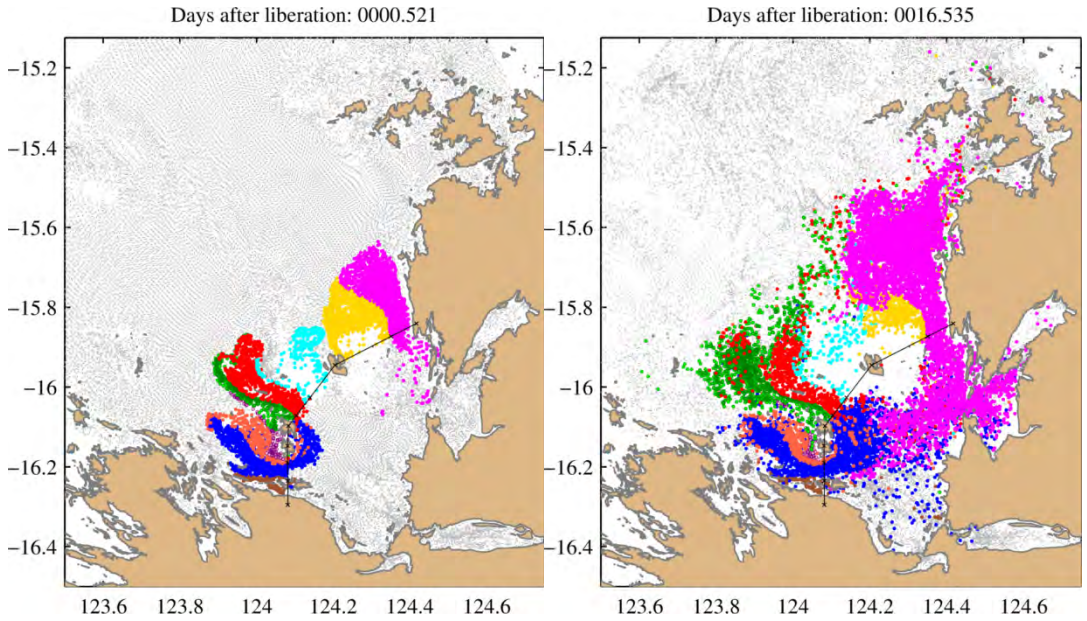

Figure 24 Series of snapshots of Lagrangian particles showing the sections where they have crossed the boundary (black line) for the fully forced simulation. All snapshots are for a slack condition at the end of ebb for the (a:) 1st cycle, (b) 32nd cycle, after release. Particles were marked with colours as in Figure 23.

3.8 Coastal flushing times

The flushing and retention times of the bay are key measures for ecological management. Clearly there are complex exchange mechanisms and here we examine the overall effects of these mechanisms and the residual circulation on bay-scale flushing. The most important period is during the dry season, which occupies much of the year and is hence the focus here. In order to measure these time scales, we follow two quite different approaches. The first approach utilizes the dilution of a passive scalar and both a global and a local flushing time can be determined. The second approach uses the particle dynamics from which a particle retention time can be obtained, and the details are in Espinosa-Gayosso et al (2016).

To estimate scalar flushing, the flow was seeded with a passive scalar with an initial concentration $C_0 = 1$ within the control volume and a value of $C_0 = 0$ outside of this region, and these initial values were set for the entire water column. A value of $C_0 = 0$ was applied at the open boundaries and for the fresh water input, if any. The northern boundary of the control volume is not identical to the boundary used in channel flux analysis above, but was displaced slightly northwards away from the jet-influenced zone in order to avoid the intense recirculation that occurs through the channels before water ultimately moves towards the open ocean, as observed in Figure 24, for example. The initial condition was set at the beginning of flood during spring tides in September 21, 2013 as representative of the dry season.

Following Juon et al (2006), a global flushing time is calculated as the time for the concentration to decrease to

35% of the initial concentration at the start of the simulation. Due to differences in the response over the bay, many locations take a finite time before there is any decrease in local concentration – a hydrodynamically induced lag effect. To account for this time lag effect, the second method waits until there is an observed decrease in local concentration, then calculates the local e-flushing time as the subsequent time needed for the concentration to then decay to 35% of the initial value – effectively a local e-flushing time (see Zhang et al (2012)). The results are shown in Figures 25a,b. Finally, a particle retention time can also be estimated for the particles, and the results are shown in Figure 25c.

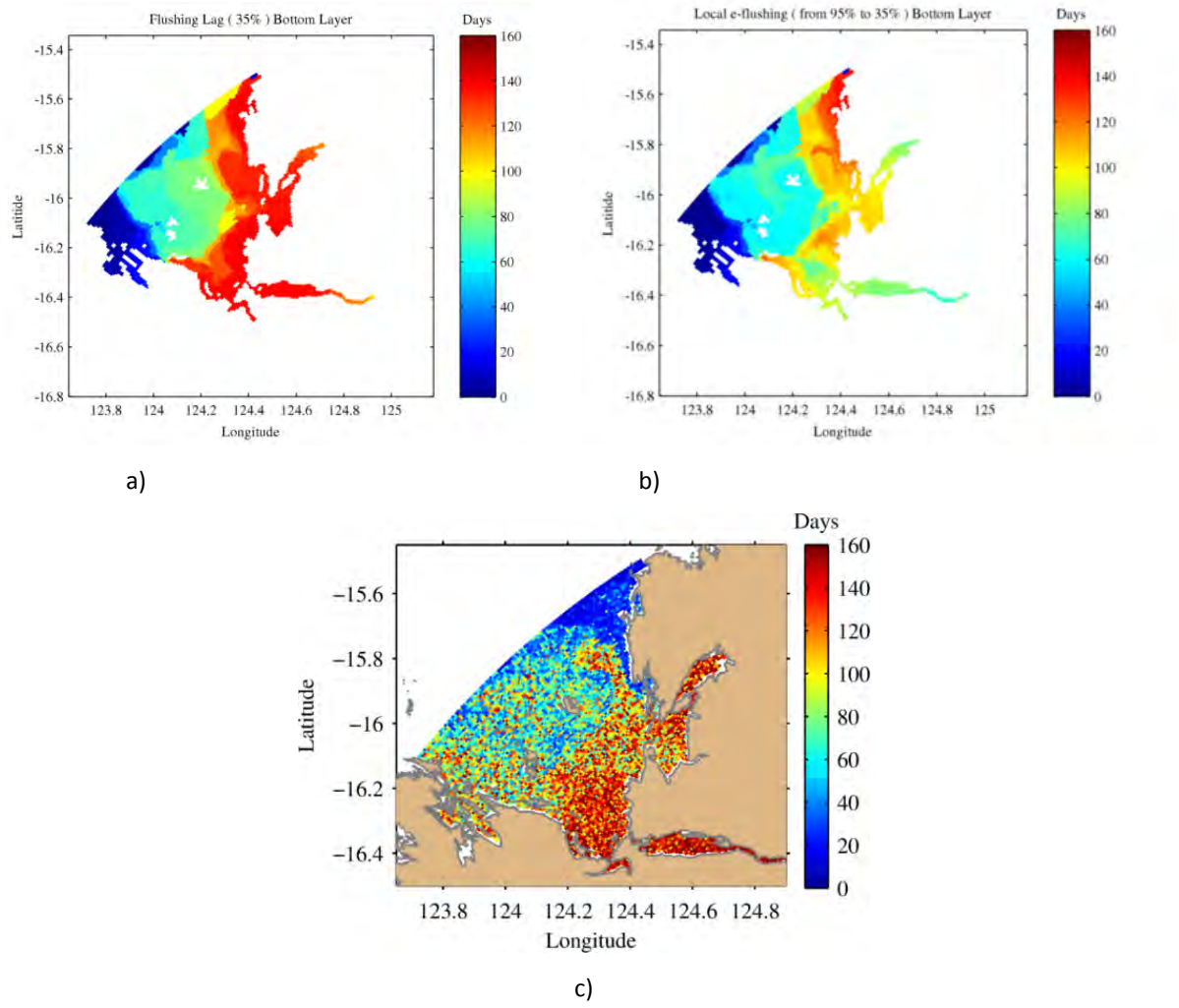

Figure 25 Flushing and retention times at Collier bay during the dry season. a) tracer global e-flushing time b) tracer local e-flushing time, c) particle retention times, liberated at the start of flood in this example.

The general trends for the two scalar flushing methods are similar, with the global flushing times (Figure 25a) and the local e-flushing times (Figure 25b) being similar in magnitude and spatial variability. The western region shows the lowest flushing times of less than 20 days, reflecting the dilution associated with the incoming oceanic water seen in the residual circulation. Because of this effective inflow, there is little lag and hence the flushing times are very similar in the western region in both Figures 25a and 25b. At the centre of the bay, intermediate values of flushing times of order 60 days are observed, while the highest values of 100-140 days occur along the eastern region. The lag effects are stronger on this eastern side, hence the differences in spatial detail between Figures 25a and 25b. The coastal estuaries and areas like Walcott Inlet show a lower e-flushing time than the eastern coast of around 80 days and can also be influenced by any incoming fresh water from the rivers at the beginning of the wet season.

The Lagrangian retention time represents the time needed for particles, liberated at specific locations, to exit the control volume. The seeding domain and the release time for the particles was exactly the same as for the scalar dilution analysis. Particles were liberated at every horizontal cell of the domain and over several vertical layers, and the result is shown in Figure 25c. Retention times are in the range from 20 to 140 days, similar numbers to the dilution analysis, but the spatial details are very different. For example, at the eastern edge, there is a long thin zone close to the coast with retention times of only 10 days. As particle-tracking movies show, the particles released in this zone are pumped out rapidly, reach the front identified in Jones et al (2014), and then move west towards the open ocean with the Bonaparte current, and never return to the Bay. Conversely, particles from the western region are transported towards the interior of the bay leading to retention times of typically 60 days on average. In general higher retention times are observed in the interior of the bay, gradually changing from ~70 days close to the jet-influenced zone to 140 days in the estuaries. Espinosa-Gayosso et al (2016) describe the details of the modeling and these outcomes.

4 Discussion and Conclusions

On a localized reef scale, an intensive study on Tallon Reef examined the hydrodynamics of this intertidal reef platform. During the flood phases of the tide, reef water levels closely followed the quasi-sinusoidal changes in offshore (i.e. off reef) water levels. However, during ebb phase, water levels over the reef lagged behind the offshore ocean and the water drained much slower off the reef compared with the returning water during flood phase. There is a substantial asymmetry between the ebb and flood currents over the reef, both in magnitude and duration. These asymmetries in the magnitude, duration and spatial pattern of the tidal flows generate residual flows every tidal cycle. The numerical model developed using SWASH was able to accurately describe the tidal hydraulics on Tallon reef, including these large ebb-flood asymmetries in both water level and currents and the details are described in Lowe et al. (2015a).

Lowe et al. (2015b) also developed a more general framework for predicting the hydrodynamics of intertidal reef platforms. In particular, the analytical model developed in that study reveals how tidal draining is dependent on properties of the reef morphology, tidal range, and the reef bottom roughness characteristics. The model was found to able to accurately reproduce the water depth decay for a wide range of physically probable bottom drag coefficients C_d and reef width L_r values. This provides physical insight into how very productive reef ecosystems living within the intertidal zone of reefs in the Kimberley, high above the offshore low tide elevation, can remain submerged (and hence survive) over a full tidal cycle.

On the regional scale, the Collier Bay/Camden Sound region was chosen to represent the extreme tides of the western Kimberley area. The field observational program in this region involved both long-term moorings and two short-term ship-based field surveys, one in the dry and the second in the wet season. The long-term deployment of three oceanographic moorings in Collier Bay/Camden Sound at the inner (35m local depth), mid (55m local depth) and outer Bay (45m local depth) locations revealed the annual tidally dominated dynamics. The M2 and S2 tidal components dominate with spring tidal ranges of 12m and neap tidal ranges of 2m. The magnitude and direction of the tidal current ellipses varied strongly over the three moorings, but even the inshore mooring was recording depth-averaged currents of up to 1m/s with greater values at the other two moorings. The strong tidal currents and the induced bottom-generated water column turbulence meant the water column was well mixed in temperature and salinity during the dry season. During the relatively short wet season, the catchment-derived freshwater input created a salinity reduction in the coastal surface layers of up to 1 pss lasting for about 60-90 days and this was diluted and transported over the Bay (Jones et al 2014).

A Regional Ocean Modelling Systems (ROMS) three-dimensional hydrodynamic numerical model for the Camden Sound/Collier Bay region was developed using the detailed bathymetry, forced by the tidal components and the wind, along with heating at the free surface, and allowing freshwater input during the wet season. The model was evaluated and tested using the three mooring observations. The model predictions of temperature, salinity, depth-averaged currents and the vertical distribution of currents over the depth were all in excellent agreement with the observations. Importantly this gives considerable confidence in the use of the model to predict processes over the entire region and as a tool to describe regional scale circulation and flushing.

The model shows that in the coastal Kimberley waters the effects of wind-forcing and density-driven forcing due to wet season fresh water input are both of only secondary importance. The dominant forcing is the tide and in particular the M2 tide with a 12.4hr period. The strong tidal forcing creates strong currents and the turbulence,

generated by the currents passing over the hydraulically rough bottom, ensures the water column is near well mixed up to depths of approximately 50m. This macrotidal forcing along with the complex topography/bathymetry of the islands and reefs are the two dominant factors that control horizontal flows and in some locations depth-averaged instantaneous currents can reach as high as 3 m/s. The flows reverse direction every half tidal period but because of the complex topography/bathymetry net or residual flows are observed on time scale longer than the tidal period.

The model shows that, in broad terms, there is a slow anti-clockwise residual circulation with oceanic water entering from the west and exiting from the north east, but the residual circulation is highly spatially variable. Due to the flow restrictions of the reef/island channels, highly energetic jets can be locally generated at each tidal cycle that reverse direction every tidal cycle locally pumping water masses (and suspended or biological matter) both in and out of the coastal region. This tidal pumping is the underlying mechanism that drives the residual circulations and their complexity reflects the complexity of the underlying topography/bathymetry. Residual depth-averaged velocities can, nevertheless, reach as high as 1 m/s, particularly over shallow reefs and in narrow channels, but varying strongly in space.

The complex residual circulation drives flushing and the mechanisms and flushing times vary across Camden Sound/Collier Bay. There is no single unambiguous way to estimate flushing in such a complex system, and different methods involving either the dilution of passive tracers or particle retention times were both used. Not surprisingly, the results are not identical but are broadly consistent and the tracer flushing tests are essentially the easiest to interpret. The dry season occupies most of the annual cycle and the mechanism of flushing is from open ocean water entering and diluting the coastal waters. The flushing times vary strongly across the Bay: from less than 20 days on the western side, between 60-80 days for the central region, and up to 120-140 days for the eastern side and the small estuaries. Thus there is a near 7-fold variation in flushing times across the Bay, but the Bay-scale average for flushing times is around 60-80 days. During the wet season some regions are additionally flushed by fresh water input from the catchment, reducing local flushing times by up to 50%, but this is strongly dependent on the location and the duration and intensity of the inflows from the catchment.

This description of the physical oceanographic dynamics in the coastal Kimberley, in turn, strongly influences the biological processes described in Project 2.2.2 and other parts of the KMRP.

5 References

Dyer, K.R. (1997) "Estuaries: A Physical Introduction", *Wiley & Sons*, 2nd Ed., Vol. 1.

Espinosa-Gayosso, A., Ivey, G.N., Jones, N.L., Lowe, R.J. and R. Brinkman (2016) Numerical study of a macrotidally forced flow in complex topography: Collier Bay, Kimberley, Western Australia, *Estuarine, Coastal and Shelf Science, in preparation*

Giddings, S.N., Monismith S.G., Fong D.A. and Stacey M.T. (2014) Using Depth-Normalized Coordinates to Examine Mass Transport Residual Circulation in Estuaries with Large Tidal Amplitude Relative to the Mean Depth, *Journal of Physical Oceanography*, V44, 128-148.

Li C. and O'Donnell J. (1997) Tidally driven residual circulation in shallow estuaries with lateral depth variation, *Journal of Geophysical Research*, V.102, N. C13, 27915-27929.

Lowe, R.J., A.S. Leon, G. Symonds, J.L. Falter and R. Gruber (2015a). The intertidal hydraulics of tide-dominated reef platforms, *Journal Geophysical Research Oceans*, doi 10.1002/2015JC010701.

Lowe, Ryan J., and James L. Falter (2015b). Oceanic Forcing of Coral Reefs. *Annual Review of Marine Science* Vol 7 (2015b).

Jones, N.L., Patten, N.L., Krikke, D.L., Lowe, R.J. and G.N. Ivey (2014) Biophysical characteristics of a morphologically-complex macrotidal coastal system during a dry season, *Estuarine, Coastal and Shelf Science*, 149, 96-108. [*Analysis of data partially funded by WAMSI 2.2.1l*]

Jouon A., Douillet P., Ouillon S and Fraunie P. (2006) Calculations of hydrodynamic time parameters in a semi-opened coastal zone using a 3D hydrodynamic model, *Continental Shelf Research*, 26, 1395-1415.

Pawlowicz R., Beardsley B. and Lentz S. (2002) Classical tide harmonic analysis including error estimates in MATLAB using T-TIDE, *Computers and Geoscience*, V.28, p9.

Stacey M.T., Burau J.R. and Monismith S.G. (2001) Creation of residual flows in a partially stratified estuary, *Journal of Gephysical Research*, 106, C8, 17013-17037.

Zhang Z., Falter J., Lowe R and Ivey G. (2012) The combined influence of hydrodynamic forcing and calcification on the spatial distribution of alkalinity in a coral reef system, Journal of *Geophysical Research*, V. 117, C04034.

6 Acknowledgements

This project was funded by the Western Australia Marine Science Institution (WAMSI) as part of the WAMSI Kimberley Marine Research Program (Project 2.2.1), and an Australian Research Council (ARC) Future Fellowship grant (FT110100201) to RJL. Our team would like to acknowledge the Bardi Jawi people, the Traditional Owners both past and present, who continue to care for this country.

7 Communications

7.1 Students supported

UWA PhD student Lei Tien (Jones, Ivey, Lowe supervisors) Structure and variability of the circulation in a macrotidal coastal system: the Kimberley, Western Australia, expected completion 2017

UWA PhD student Wencai Zhu (Jones, Espinosa, Hipsey supervisors) Wet season hydrodynamics in and physical/biological interactions in the Kimberley, expected completion in 2017.

UWA Honours student Joshua Garlepp (Jones supervisor). Oceanography of the Kimberley: a preliminary study of the circulations patterns in Walcott Inlet and surrounding Camden Sound 2015

7.2 Journal publications

Jones, N.L., Patten, N.L., Krikke, D.L., Lowe, R.J. and G.N. Ivey (2014) Biophysical characteristics of a morphologically-complex macrotidal coastal system during a dry season, *Estuarine, Coastal and Shelf Science*, 149, 96-108. *[Analysis of data partially funded by WAMSI 2.2.1]*

Lowe, R.J., A.S. Leon, G. Symonds, J.L. Falter and R. Gruber (2015a). The intertidal hydraulics of tide-dominated reef platforms, *Journal Geophysical Research Oceans*, doi 10.1002/2015JC010701. *[The focus is on the hydrodynamics at the intertidal reef on Tallon Island, project funded by WAMSI 2.2.1]*

Lowe, Ryan J., and James L. Falter. Oceanic Forcing of Coral Reefs. *Annual Review of Marine Science* Vol 7 (2015b). *[While not the primary focus of this review article, the Kimberley reefs were featured as a case study and example of tide-dominated reefs that have remained poorly studied globally].*

Branson, P.M., M. Ghisalberti and G.N. Ivey (2016) Time resolved 3D3C measurements of shallow-water island wakes, *Proceedings 20th Australasian Fluid Mechanics Conference*, Perth, 5-8 December 2016. *to appear*

Zhou, W., M., Espinosa-Gayosso, Jones, N.L. and M.R. Hipsey (2016) Numerical study of the wet-season hydrodynamics of a macrotidally forced bay with complex topography: Collier Bay, Kimberley, Western Australia. *Proceedings 20th Australasian Fluid Mechanics Conference*, Perth, 5-8 December 2016.

Espinosa-Gayosso, A., Ivey, G.N., Jones, N.L., Lowe, R.J. and R. Brinkman (2016) Numerical study of a macrotidally forced flow in complex topography: Coller Bay, Kimberley, Western Australia, *Estuarine, Coastal and Shelf Science*, *in preparation*

7.3 Presentations

R. Lowe presented a paper at the AGU/ASLO Ocean Sciences meeting in Hawaii in February 2014. Title: Hydrodynamics of the macrotidal reef systems in north western Australia" [*funded through 2.2.1*]

M. Furnas, presented a paper at the AGU/ASLO Ocean Sciences Meeting in Hawaii in February 2014. Title: High phytoplankton productivity in hyper-physical tropical shelf and coastal system: the Kimberley shelf, NW Australia, [*Used physical data provided through 2.2.1*]

G. Ivey presented a paper at ACOMO 2016 in Canberra, October 2016. Title: Sub-mesoscale dynamics on the Australian North West Shelf (NWS) from Ningaloo to the Kimberley. [*Includes data and modelling done through 2.2.1*]

P. Branson presented a paper at the 20th AFMC in Perth, December 2016. Title: Time resolved 3D3C measurements of shallow-water island wakes. [*A laboratory modelling study motivated by field work and numerical modelling work done in 2.2.1*]

Wencai Zhou presented a paper at the 20th AFMC in Perth, December 2016. Title: Numerical study of the wet-season hydrodynamics of a macrotidally forced bay with complex topography: Collier Bay, Kimberley, Western Australia. [*A numerical modelling study of wet season dynamics part of 2.2.1*]

7.4 Other communications

Brinkman, R. and M. Furnas (2014): Interview on WAMSI activities by ABC TV (Broome) in Broome prior to departure of the October 2013 Solander voyage. Portions of the interview were broadcast locally and nationally on the ABC24 news channel.

http://mobile.abc.net.au/news/2013-10-23/marine-science-study-begins-off-kimberley-coast/5041534?section=business

Appendix 1. This project directly addresses the following questions outlined in the Kimberley Marine Research Program Science Plan and in the project Agreement.

Key Question	**Informed Response**
What feeds the system - is it the catchment or is it the ocean – does this change by season?	The ocean feeds the system throughout the year. During the wet season, there is freshwater input from the catchment to the near-coastal waters, but this is secondary compared to the ocean exchange.
Are there large spatial (e.g. inshore-offshore) and temporal (e.g. tidal, seasonal, inter-annual) variations in productivity in the water column in this region?	There are large horizontal spatial and temporal variations in physical processes and these should, in turn, promote variations in productivity.
What physical (e.g. macro-tidal forcing and freshwater input from wet to dry season) processes (spatially and temporally) are 'driving' this observed variation in biological activity?	The effects of wind and freshwater input are secondary and relatively weak. The dominant physical processes are the tidally-induced horizontal flow and vertical turbulent mixing.
How are large-scale oceanic processes related to local physical and biological oceanography– cyclones (one month pulses, ENSO (12 months)	Cyclone-induced rainfall over the catchment will lead to freshwater input into the coastal waters. Cyclones and long term, large-scale oceanic processes may change offshore ocean properties, such as temperature for example, but will not affect the dominant tidally-driven flushing of the coastal waters.
How does the distribution of fauna and flora relate to large and small scale oceanographic processes?	The coral reefs in the region are hydraulically rough, this slows the local flow and hence sets the drainage of ocean waters from the reefs as the tide descends. The distribution of the coral reefs and channels thus also controls the large scale circulations patterns in the area.
How do large tides and fresh water influence inshore and estuarine ecosystems, how might modification (e.g. damming, water extraction etc) effect these ecosystems?	Freshwater influence is localised and, due to the strong vertical mixing, keeps coastal waters near oceanic salinities even during the wet season. The large tides control the flows and hence nutrient supplies to the coral reef ecosystems.
How will changes in climate (e.g. rainfall) affect tropical estuaries in terms of discharge, and how will this influence other physical processes (e.g. sedimentation)?	Potential increased rainfall due to climate change would increase freshwater inputs from catchments and estuaries. However, the strength of the tidal flows will be unaffected by climate change.
What is going on with sedimentation – its role in productivity and flux based on water flow?	The tidally-induced vertical mixing is so strong that it will keep sediment well mixed over the vertical column, and this, in turn, sets light penetration and hence productivity in the water column.
How might we best measure changes in physical and biological oceanography, particularly in relation to climate change?	Monitoring of long-term changes in rainfall and freshwater input from the catchment would be useful. Similarly long-term measurements of offshore water temperatures would be recommended.
What will be the trajectory of oil spills under typical oceanographic conditions? (Broad statements)	Within the area of this study in Camden Sound/Collier Bay, oil spills would likely follow the residual circulation from offshore into the bay in the west and then exiting to the north east, with a likely residence time of the order of months.
How does physical oceanography of the Kimberley inform our understanding of connectivity?	It determines connectivity. Wind may influence material or tracers which exist only at the free surface, but connectivity

	of waters over the water column will be controlled by the strong tidal flows.
What is this project adding to our understanding of bathymetry across the Kimberley?	Bathymetry and its complex spatial variability controls the physical oceanography.
How applicable will this information be to areas where there is a lower tidal difference (ie across the whole region)? What is going on in Roebuck Bay?	The same methods of analysis can be applied anywhere in the Kimberley. As the tidal amplitude decreases, so will both the strength of the horizontal flow and the vertical mixing. The local details will depend strongly not just on the reduced tidal flow, but also on the local bathymetry and particularly the extent of the coral reef systems.
What can managers keep an eye on to understand changes in the system and respond? What is the best practical descriptor for major oceanographic changes in the Kimberley (better than sea level at Freo)?	Monitoring ocean temperature and rainfall, and monitoring potential pollutant releases or spills.
What will we be able to manage/how will we best use this information?	The knowledge can be used to manage proposed development by industry or community in the region, and to inform best response for unforeseen hazards or events.